Fachbereich Erziehungswissenschaft und Psychologie
der Freien Universität Berlin

# Context-Dependent Modulation of Value Processing in the Human Brain

Dissertation

Zur Erlangung des akademischen Grades
Doktorin der Philosophie (Dr.Phil.)

Vorgelegt von

Dipl. -Psych. Park, So Young

Berlin, 2011

**Erstgutachter/in**
**Professor Dr. Hauke R. Heekeren**

**Zweitgutachter/in**
**Professor Dr. Jörg Rieskamp**

Disputationsdatum: 10. Februar 2012

*To my family*

## Acknowledgements

I wish to thank first and foremost my supervisor Prof. Hauke Heekeren, who patiently guided, supported and challenged me whilst allowing me the room to work in my own way. I sincerely appreciate his trust in me throughout the whole PhD process, which has shaped and formed my scientific work. I would like to also thank my co-supervisor Prof. Jörg Rieskamp for teaching me to see things from different perspectives. He showed me the joy of being open to discussion, to question and 'to play' by doing science. I thank Prof. Raymond Dolan for his warm support, for the inspiring discussions and especially for teaching me how to write.

Special thanks for the funding, teaching and support to the Berlin School of Mind and Brain. It was an honour to be a student of this great school. The school provided a stimulating context that widened my scientific understanding in many ways. Especially to Annette Winkelmann, for all her support with the many questions and challenges a PhD student can encounter. I thank my parents and my brother for their trust and never-ending love. Finally, it is difficult to put into words the debt that is owed to Thorsten Kahnt, for his patience and willingness to carry out scientific discussions day or night. His advice, steady support and endless encouragement both in science and in life have pushed me to achieve goals of which I did not believe I was capable. Without you I would not be what I am now.

## Table of Contents

## Zusammenfassung

Viele Alltagsentscheidungen basieren auf Belohnungswerten. Entscheidungsoptionen wie ein Dessert, Urlaubsziele, ein neues Paar Schuhe usw sind mit gewissen positiven Werten assoziiert. Allerdings ist es nicht der Belohnungswert allein, den wir betrachten, um Entscheidungen zu treffen. Vielmehr betrachten wir diese Werte in einen Kontext eingebettet. Beispielsweise sind die Preise der Schuhe oder die Kosten des Urlaubs negative Werte die den Kontext darstellen. Kontextabhängigkeit besteht auch, wenn die Werterwartungen mit dem tatsächlichen Wert verglichen werden. Die Berechnung eines Erwartungsfehlers (Prediction Error, PE), also die Differenz zwischen dem erwarteten und dem tatsächlichen Wert, wird der Belohnungshöhe angepasst. Diese Kontextabhängigkeit ist essenziell für erfolgreiches Entscheidungsverhalten, da diese die Berücksichtigung des gesamten Belohnungsbereichs ermöglicht und gleichzeitig die Sensibilität für kleinste Veränderung garantiert. Für diese Dissertation habe ich zwei Experimente durchgeführt, um die neuronalen Korrelate von kontextabhängiger Wertverarbeitung zu untersuchen. Insbesondere wurden hier die zwei folgenden Kontexte untersucht: negativer Wert und Belohnungshöhe. Dafür wurde die Hirnaktivität von gesunden Probanden mit funktioneller Magnet-Resonanz-Tomografie (fMRT) erfasst. Diese Daten wurden mithilfe von mathematischen Modellen und funktionellen Konnektivitätsanalysen ausgewertet. Die Ergebnisse des ersten Experiments zeigen, dass positive Werte mit den assoziierten negativen Werten interagieren und nicht nur additiv integriert werden. Dieser Prozess wird mit einer Veränderung der Konnektivität zwischen dem subgenualen anterioren Cingulum (SGACC) und der Amygdala in Verbindung gebracht. In dem zweiten Projekt wurde untersucht, wie die Kodierung von Erwartungsfehlern unterschiedlichen Belohnungshöhen angepasst wird. Die Ergebnisse zeigen, dass die Erwartungsfehler für hohe und niedrige Belohnungen indifferent sind. Des Weiteren stellte sich heraus, dass diese Anpassung durch eine Veränderung der Konnektivität zwischen dem präfrontalen Kortex sowie dem Mittelhirn und dem Striatum implementiert wird. Hierbei war die Konnektivität bei hohen Belohnungen geringer ausgeprägt als bei niedrigen Belohnungen.

Zusammengefasst zeigen die Ergebnisse der beiden Experimente, wie kontextabhängige Wertverarbeitung im menschlichen Gehirn implementiert wird. Diese Ergebnisse erweitern unseren Wissensstand bezüglich der neuronalen Verarbeitung von Werten, die menschlichem Entscheidungsverhalten zugrunde liegen.

**Summary**

Everyday choice options are based on reward. We associate decision options such as a dessert, a holiday destination, a new pair of shoes with certain subjective reward values. However, it is not only the reward value alone that influences our decisions. These values are considered in certain contexts. For example, the price of the shoes or the costs of a vacation are negative values associated with the reward value and serve as contexts. Also, the computation of prediction errors (PE) is context-dependent. PE refers to the difference between the expected and received reward and its representation adapts to the different reward magnitudes. This context dependency is essential for successful decisions making, because it enables the representation of the whole reward range and at the same time guarantee the sensibility for the smallest changes. In this thesis, I conducted two experiments to investigate the neural correlates of context-dependent modulation of reward processing. Specifically, two essential contexts were considered: negative value and reward magnitudes. To this end, brain data was collected from healthy subjects using functional magnetic resonance imaging (FMRI). Computational models and effective connectivity analyses were applied for data analysis. The results of the first experiment demonstrate positive and negative values are integrated interactively and not only additively. This interactive process is accompanied by changes in connectivity between the subgenual anterior cingulate cortex (SGACC) and the amygdala. In the second project, the reward-magnitude dependent adaptation of prediction errors was investigated. The results demonstrate that the striatal coding of prediction errors is indifferent for high and low rewards. Furthermore, this adaptation is implemented by striatal connectivity changes with the medial prefrontal cortex (MPFC) and the midbrain.

In summary, the results of the two experiments in this thesis show how context-dependent value processing is implemented in the human brain. These results extend our understanding of neural processing of value underlying human decision making.

## List of original publication

This thesis is based on the following original research articles:

Project I

Park, S.Q., Kahnt, T., Rieskamp, J., Heekeren, H.R. (2011)

Neurobiology of value integration: When value impacts valuation.

*J Neurosci*, 31(25): 9307-9314

doi: 10.1523/JNEUROSCI.4973-10.2011

Project II

Park, S.Q., Kahnt, T.,Talmi, D., Rieskamp, J., Dolan,R.J., Heekeren, H.R. (2012)

Adaptive coding of reward prediction errors is gated by striatal coupling.

*Proceedings of the National Academy of Sciences (PNAS), in press*

doi: 10.1073/pnas.1119969109

## List of abbreviations

BOLD Blood Oxygen-Level Dependent

FMRI Functional Magnetic Resonance Imaging

HRF Hemodynamic Response Function

GLM General Linear Model

PPI Psycho-Physiological Interaction

PE Prediction Error

SN Substantia Nigra

VTA Ventral Tegmental Area

SGACC Subgenual Anterior Cingulate Cortex

OFC Orbitofrontal Cortex

MPFC medial Prefrontal Cortex

VMPFC Ventromedial Prefrontal Cortex

# 1. Introduction

## 1.1 General Overview

In everyday life, we encounter many different decision options; what to eat for dinner, where to go for vacation, whether to eat another piece of chocolate. These options are associated with certain reward values. However, when making decisions, we do not rely on the reward value alone. Instead, the reward value is considered in a certain context and this context modulates the valuation process. For example, when deciding among desserts, we put the reward value of the taste in relation to its price. Here, the context is the cost, like the monetary price or the perspective of gaining weight that is combined with, and can modulate the reward value.

Reward magnitude is another important context that modulates value processing. From receiving a piece of chocolate to winning the lottery, the range of possible rewards in the world is immense, yet the firing range of reward-sensitive neurons is limited. An efficient way for the brain to solve this problem is by dynamically adjusting the activity range of neurons according to the context. Such an adaptive coding mechanism maximizes the discriminability between different values in a given reward context, thus enabling efficient information processing.

Within a small fraction of time, our brain represents all the different aspects coupled with value and computes the subjective value with respect to its context. How is this context-dependent reward processing implemented in the brain? What is the underlying mechanism? Although reward coding and reward anticipation in the human brain have been widely investigated (Montague and Berns, 2002;Rangel et al., 2008;Glimcher and Rustichini, 2004;Peters and Buchel, 2010), it is not clear how our brain actually processes value-related information in different contexts. This is partly due to the fact that its investigation is

challenging, because different from the mere representation of reward value, value processing is a dynamic computational process and subjective, hence not easily observable.

In this dissertation, I present the results of two experiments that investigate the neural mechanisms of context dependent valuation. Here, I focus on two reward modulating contexts that are essential for making decisions: 1) the reward valuation process in the context of negative value (cost) and 2) the prediction error (PE) computation (i.e. the mismatch between predicted and received reward) in the context of different reward magnitudes (large or small reward). To investigate the underlying mechanisms, I apply computational modelling and functional connectivity analysis to human brain data obtained by functional magnetic resonance imaging (FMRI).

The first study shows that when integrated together, the negative value (i.e. cost) impacts reward value interactively and not only additively (Park et al., 2011). The results of this study explain to what degree we perceive expensive products as more valuable and appreciate rewards resulting from hard work more than easily obtained rewards. The second study shows how we compute prediction errors in the context of different reward magnitudes (Park et al., revised manuscript). The results show a mechanism that enables the flexible adaptation of prediction errors to the momentarily available reward magnitude: A context dependent process that facilitates successful decision making and learning with rewards in all sizes in every situation.

In the first chapter, I will summarize the theoretical background of reward and previous findings on the neurobiology of reward. The second chapter encompasses a brief, conceptual introduction to the methods used in this thesis. The two experimental studies will be introduced in more detail in chapter 3. Finally, chapter 4 will discusses the results of

the two studies. Based on these results I will propose a neurobiological model of context-dependent value coding as well as how this model can be tested in future experiments.

## 1.2 Reward and reinforcement learning

Reward modifies and shapes our behaviour. The psychologist Edward Thorndike (Thorndike, 1911) introduced a basic learning mechanism: the law of effect, which states that every behaviour, leading to a pleasant event (or to the termination of an unpleasant event), is more likely to occur again. Skinner (Skinner, 1938;Skinner, 1953) defined this as reinforcer in his theory of operant conditioning: in a given situation, every stimulus following a certain behaviour, is a positive reinforcer when it leads to an increase in the probability of this behaviour. In contrast, when the removal of the stimulus leads to an increase of the behaviour, this is considered as a negative reinforcer. Both Thorndike's and Skinner's theories describe the mechanism of reinforcement learning to maximize reward and minimize punishment. In contrast, classical conditioning describes the procedure of how an initially neutral stimulus (CS) acquires predictive value about a reward (US) via repeated simultaneous or subsequent presentation (Pavlow, 1927). Here, no instrumental behaviour is required, although after learning, the CS can elicit the same reward related responses as the US.

This mechanism of reinforcement learning has been formalized using mathematical equations (Rescorla, 1972;Jungermann, 1976;Sutton and Barto, 1998). The basic assumption is that reinforcement learning relies on prediction errors. Prediction errors are the discrepancy between the predicted and actually received reward outcome and are thought to act as a teaching signal to update the value of the CS. When the action/cue - outcome association is newly introduced, the prediction error is large. However, with repeated pairings of the action/cue and the outcome the value of the action/cue increases and the prediction error will become smaller and eventually diminish, meaning the action/cue can fully predict the reward outcome and learning is completed.

This concept of prediction error has received wide attention and played an essential role in elucidating the neurobiology of learning and reward-based decision making in the brain (Schultz et al., 1997;O'Doherty et al., 2006;Pessiglione et al., 2006;Seymour et al., 2005;Park et al., 2010;Kahnt et al., 2009).

### 1.3 Neural representation of reward

In the last decades, there have been immense efforts to investigate the neurobiology of reward processing across species. Specifically, human FMRI studies have suggested the involvement of the ventral striatum, the amygdala and the prefrontal cortex including the orbitofrontal cortex (OFC in reward processing (Knutson et al., 2001b;Breiter et al., 2001;O'Doherty, 2007;Kahnt et al., 2010). These studies applied both primary rewards such as food or drinks (O'Doherty et al., 2002;Francis et al., 1999;Aharon et al., 2001;Kringelbach et al., 2003) and secondary rewards such as money to investigate reward representations in the human brain (Knutson et al., 2001a;O'Doherty et al., 2001;Elliott et al., 2003;Blood et al., 1999).

Choice options can be of the same or of different types of reward. i.e. we are able to decide among dinner menus, but we can also decide between going to the opera or to an elegant restaurant for dinner. Although the nature of rewards is very different, we are able to flexibly compare or combine them. According to the observation that different reward types such as money, food or even social rewards such as attractive faces or erotic pictures are coded in shared brain networks , it has been suggested that the brain encodes different reward types by transforming them into a common value currency (Montague and Berns, 2002;Glimcher and Rustichini, 2004;O'Doherty, 2007;Sescousse et al., 2010;Smith et al., 2010). In line with this, recent experimental studies have directly compared different types of rewards, such as food, juice, consumables and monetary gambles. These results demonstrated that all these rewards are represented in the same region, namely the ventromedial prefrontal cortex (VMPFC) (Chib et al., 2009;Kim et al., 2011;Levy and Glimcher, 2011).

### 1.4 Brain mechanisms of context dependent reward processing

Although the neural representation of reward has been well investigated during the last decade, it is not clear how the valuation process changes depending on the context. Previous research on the neurobiology of reward-based decision making has mainly focused on reward options that are presented alone, such as monetary reward. However, in everyday decision situations, values are mostly embedded in contexts and are not presented in isolation. Therefore it is inevitable for the brain to flexibly adapt value representation according to its context. On the neural level, it can be assumed that such dynamic process is implemented not only by the activation of a single brain region, but in the modulation of the coupling across multiple regions. Hence, it is important to consider multiple neural systems carrying out different valuation mechanisms.

Several primate studies have demonstrated that neurons adaptively code reward values in different contexts. Midbrain dopaminergic neurons adapt to different reward magnitudes when representing prediction errors. Specifically, these neurons increase their activity for the larger of two potential reward outcomes and decrease their activity for the smaller outcome independent of the absolute reward magnitude (Tobler et al., 2005). Reward coding OFC neurons adapt their firing rate to reward variability (Kobayashi et al., 2010) and to the reward range (Padoa-Schioppa and Assad, 2008;Padoa-Schioppa, 2009). Furthermore, a recent study has shown that the primate lateral intra-parietal cortex codes saccade values of the same option depending on other available choice options (Louie et al., 2011). Adaptive coding can be also found in the visual system, such that our receptors adjust their coding range according to the momentarily available light intensity. This context-dependent adjustment is implemented via feedback loops involving different neurons (Dunn

et al., 2007). This suggests that context-dependent adaptation requires the interplay between multiple neuronal systems.

For decades, economic models have assumed that when a person evaluates a choice option, different values contribute independently to the overall subjective value of the option (Keeney and Raiffa H, 1976;Wallenius et al., 2008). In contrast, human choice behaviour often violates this assumption, suggesting interactions between values (Huber, 1974;Wallenius et al., 2008). For example, when choosing a dinner menu with cheese, red wine has a higher value, whereas with fish, white wine has a higher value. Here, a valuation mechanism ignoring the context would fail to predict behaviour, whereas a context-dependent interactive integration would successfully predict choices. Similar interactive mechanisms modulating hedonic experience have been demonstrated in neuroscientific studies from different areas. For example, the placebo effect or attention regulates pain perception interactively (Wager et al., 2006;Bingel et al., 2006;Wiech et al., 2008). Interestingly, these neuroscientific studies on context-dependent modulation converge onto the same brain region, namely the subgenual anterior cingulate cortex (SGACC). This region, in concert with the amygdala has been shown to be involved in modulation of pain and fear processing (Bingel et al., 2006;Wiech et al., 2008;Phelps et al., 2004).

Another fundamental question is whether prediction errors are coded in a context-dependent manner. Possible rewards in the world are immense, whereas the range of neural firing is limited. How can people with the same neural system compute the prediction error for millions of dollars on Wall Street and at the same time monitor whether their lunch is as good as predicted? In other words, how can we code the immense range of values and, at the same time remain sensitive to small differences in reward? One possibility for the brain to solve this is to dynamically adjust the activity range according to the momentarily

available rewards. This adaptive coding of reward prediction errors (PEs) has been suggested by a wide range of theories including economics and reinforcement learning. Prospect theory suggests that people apply an anchoring heuristic and changes are coded according to the individual reference outcome (Kahneman and Tversky, 1979). For example, when we win 50€ with an expectation to win 10€, there will be a prediction error of +40€. However, when our initial expectation was to win 100€, the same win of 50€ will induce the prediction error of -50€. In reinforcement learning theory, the PE is considered to be fundamental for updating the reward values associated with the predicting cue (Frank and Claus, 2006;Sutton and Barto, 1998). Adaptive coding of prediction errors is essential for two reasons. First, the reward magnitude (lottery or chocolate) is already encoded during expectation. Hence, in terms of efficient neural coding, it is not necessary to represent the reward magnitude redundantly when computing the prediction errors. Second, computation of this quantity depending on reward magnitude would prohibit learning from small rewards. That is, no matter in what situation we are, only the prediction error of extremely high rewards would be behaviourally relevant and prediction errors of small rewards would never impact behaviour.

In human FMRI studies, PEs were shown to correlate with the BOLD response in the ventral striatum (Park et al., 2010;Pessiglione et al., 2006;Kahnt et al., 2009). Furthermore, human imaging studies have demonstrated that the striatal PE coding is adaptive (Nieuwenhuis et al., 2005;Lohrenz et al., 2007;Fujiwara et al., 2009). Although adaptive coding in reward-sensitive neurons is well documented (Tobler et al., 2005;Tremblay and Schultz, 1999;Padoa-Schioppa, 2009;Kobayashi et al., 2010) it remains an open question how the brain implements the normalization process, bringing different magnitudes onto the same coding scale. The striatum receives major dopaminergic projections from the midbrain

and both striatum and midbrain are tightly interconnected with prefrontal cortex (Sesack and Pickel, 1992;Sesack et al., 1989;Haber and Knutson, 2010;Haber et al., 2000;Haber et al., 1995;Haber and McFarland, 1999). Hence, the PFC and the midbrain seem to be major candidate regions for context-dependent adjustment of the striatal PE signal.

Computational mechanisms such as context-dependent modulation of value processing are not easily observable at the behavioural level. It is also very likely that such complex processes are expressed not only by the activity of a single brain region, but by dynamic changes in the connectivity among multiple brain regions that have different functions. Recent developments in FMRI have led to new analysis methods that enable us to gain insight into such brain mechanisms. In the following section, I will provide an overview about two methods, namely model-based FMRI analysis and psycho-physiological interaction as effective connectivity analysis. Both methods were applied to analyze the FMRI Data of the two experiments presented in chapter 3.1 and 3.2.

# 2. Methods: Model-based FMRI and effective connectivity

## 2.1 Model-based FMRI

A well established approach to investigate computational processes underlying decision making is to use cognitive models (Mazur and Biondi, 2009;Navalpakkam et al., 2010;Bhatt et al., 2010). A cognitive mechanism or process can be explicitly formulated using a mathematical model. These models can then be tested by comparing model predictions on behavioural data. This allows us to gain insight into the underlying computational mechanism of the cognitive process in question. However, applying computational models not only to behavioural data, but also to neural data has several benefits. First, this method can provide direct evidence about the neurobiology underlying the cognitive process. Here, instead of using the model's output to predict the behavioural data, the hidden variables of the model can be used to predict brain data. This provides information about 'where' in the brain 'which' specific mechanism is implemented. Second, by comparing the degree to which brain activity can be accounted for by different competing models, it is possible to show that the brain data is better explained by one model over the other. Thus, the brain data provides a mean to discriminate between different computational models of cognitive functions.

Model-based FMRI refers to applying cognitive models to brain data obtained with FMRI. The analysis typically begins with fitting a computational model to subjects' behavioural responses (FIGURE 1). This process involves the estimation of optimal values of the free parameters for each subject by minimizing the difference between model predictions and subject's actual behaviour. The best model can then be selected by testing their ability to predict behaviour. Once the best model is found, its trial-by-trial computational variables are regressed against the imaging data using a general linear model (GLM). By doing so, we can identify brain regions in which activity is significantly correlated

with the model variable. This technique offers great advantage over traditional FMRI analysis methods by providing the information of 'how' a particular cognitive process is implemented in a specific brain area. In contrast, conventional FMRI analysis methods offer only the information about 'where' by unveiling brain regions showing enhanced BOLD activity while performing a specific task or condition (O'Doherty et al., 2007;Rangel and Hare, 2010).

A more elaborative approach of model-based FMRI is identifying the model that accounts best for both subjects' behavioural and FMRI data. In case competing models make similar predictions about behaviour, behavioural data are limited in selecting the best model (Bruni and Sugden, 2007). Here, forcing the models to predict neural activity helps to identify the underlying computational mechanism. In other words, imaging data provides a more fine grained and rich source of evidence that can be used to constrain different computational models (Glimcher and Rustichini, 2004;Hampton et al., 2006;Hampton et al., 2008;Kable and Glimcher, 2007;Loewenstein et al., 2008;Mohr et al., 2010).

The great advantage of model-based FMRI is that the hypotheses about cognitive mechanisms are clearly defined as mathematical equations and the quantitative model predictions are directly testable. However, when comparing the fit between models, it is important to be aware of the fact that complex models with more free parameters tend to fit the data better (Stone, 1974). Hence, it is necessary to punish the model with more free parameters when comparing the fitness of models with different numbers of parameter (O'Doherty et al., 2007). Alternatively, instead of comparing model fits, the ability of the model to predict new data can be compared (O'Doherty et al., 2007). Here, the data are split into two sets and the model parameters can be estimated based on one data set and then be tested on the other data set. This procedure can be repeated, using leave-one-out cross

validation, until all the data sets have been used to fit and to test the model (von Helversen B. and Rieskamp, 2009).

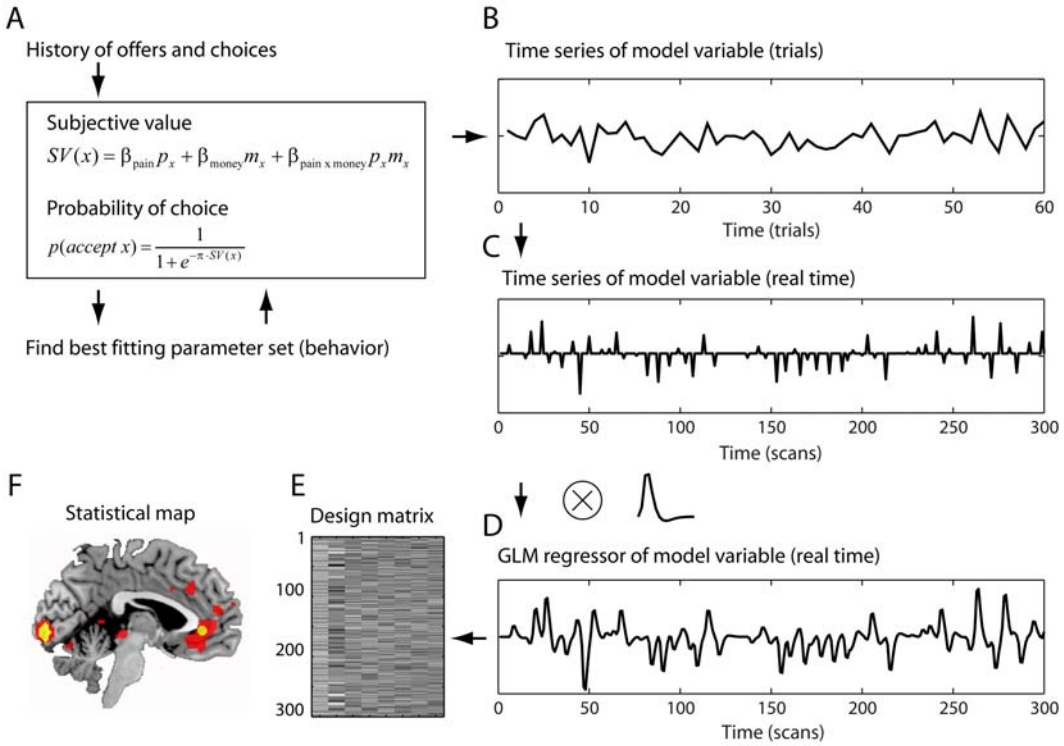


**FIGURE 1** Model-based FMRI

**A.** By maximizing the correlation between the model output (p(accept x)) and the actual choice behaviour, the model parameters can be estimated. **B.** Using these individual parameters, a regressor is created, in which trials are parametrically modulated by the model-derived subjective values (SV). **C.** A time-series is generated, by time-logging the trials to real time. **D.** The resulting regressor is convolved with a hemodynamic response function (HRF) to account for sluggishness of the BOLD response. **E.** Using a general linear model (GLM), the regressors are used to predict the FMRI data. **F.** The statistical map represents the degree of correlation between the parametric regressor and the BOLD signal in each voxel.

## 2.2 Psycho-physiological interaction analysis with FMRI data

Different from a conventional univariate FMRI-analysis, which reveals the BOLD response in certain psychological conditions, a connectivity analysis unveils how brain regions change their correlation depending on the condition (Friston et al., 1997;Gitelman et al., 2003). As its name suggests, the psycho-physiological interaction (PPI) can be considered as a factorial model, in which the main effect of the psychological variable (which captures pure task related BOLD responses), the physiological main effect (capturing the non-specific correlation with the seed region), and their interaction (reflecting task-related changes in the correlation between the activity in the seed region and other brain areas) can be tested. This method has been widely applied to investigate inter-regional connectivity modulations that accompany different cognitive states (Camara et al., 2008).

The basic procedure of PPI analysis begins with extracting the entire BOLD time course over the experiment from the seed region in each subject (FIGURE 2). The seed region can be defined either anatomically (e.g. using an anatomic atlas) or functionally. The time series (physiological factor) are first averaged across the voxels within the seed region and then undergo pre-processing steps such as high-pass filtering, global-mean normalization, removal of noise caused by subject's movement, etc. The psychological factor represents a cognitive state or task condition. To create the interaction between the physiological and the psychological factor (the PPI regressors), the time series is multiplied with condition vectors containing ones for 12 seconds after each psychological condition and zeros otherwise. The time window of approximately 12 seconds is necessary to capture the entire hemodynamic response function (HRF), which peaks after 6 seconds and is back at baseline about 14 seconds after the stimulus onset (Handwerker et al., 2004). These regressors are used as covariates in a GLM, which also contains the psychological regressors

and the entire time series of the seed region as physiological regressor. The psychological regressors are convolved with a HRF to predict the BOLD response during a condition. Importantly, all the regressors need to be regressed simultaneously, so that the shared variance can not be attributed to any of the regressors. The resulting parameter estimates of the PPI regressors represent the extent to which activity in each voxel correlates with activity in the seed region in that specific task condition. The method described above relies on correlations in the observed BOLD time-series data, and makes no assumptions about the nature of the neural event contributing to the BOLD signal (Park et al., 2010;Park et al., 2011;Park et al., revised manuscript;Kahnt et al., 2009;Pessoa et al., 2002).

It is important to note that meaningful connectivity results require the comparison between two conditions and cannot be interpreted alone. An essential pre-processing step requires global-mean normalization (the mean of all the voxels in the whole brain) to reduce non-specific correlations between brain regions. This shifts the whole-brain correlation distribution to have a mean near zero and thus forces negative correlations to appear, even if no such correlations are initially present in the data (Van Dijk et al., 2010;Murphy et al., 2009;Fox et al., 2009). Hence, the direction of the correlation cannot be interpreted, but only the size of the difference in correlations between two (or more) conditions.

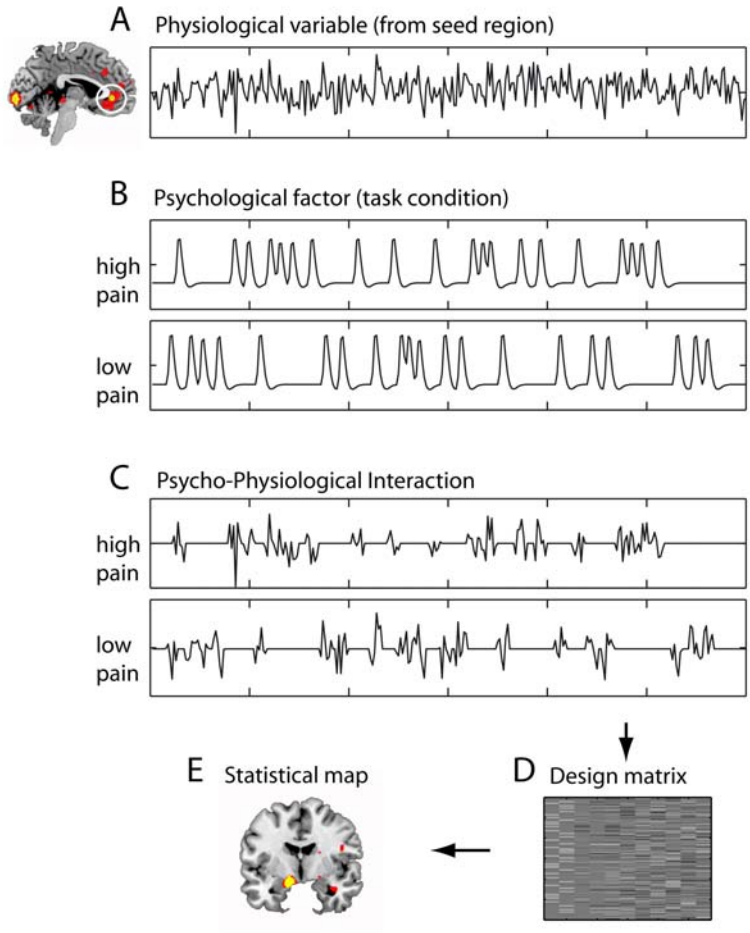


**FIGURE 2** Psycho-physiological interaction analysis (PPI)

**A.** Physiological regressor, i.e. the entire time series extracted from the seed region. This regressor captures the correlation with activity in the seed region. **B.** The psychological regressors are conventional onset regressors convolved with a HRF to predict the BOLD response during a condition. **C.** Psychological-physiological interaction term. Note that the regressors are modulated by the physiological regressor, only for 12 seconds after trial onset of each condition. **D.** All regressors are entered simultaneously into a GLM. **E.** Finally, by contrasting the PPI regressors between two conditions, statistical maps can be created. Here, the statistical brain map represents the condition-related change in the correlation between activity in each voxel and the seed region.

# 3. Experiments: Neural mechanisms underlying context-dependent modulation of reward processing

This chapter summarizes two experiments (Park et al., 2011;Park et al., revised manuscript) that constitute the main part of this dissertation. In these experiments, model-based FMRI and effective connectivity analyses were applied to investigate context-dependent reward processing. The first study compared different computational models directly on neural data and demonstrated that valuation of the very same reward is modulated depending on the combined negative value. Specifically, the neural data provided decisive information that this modulation was interactive. This interaction of different values was accompanied by changes in connectivity between the SGACC and the amygdala (Park et al., 2011). The second experiment investigated how the brain represents the mismatch between predicted and received rewards in different reward contexts. This aimed to define whether our prediction error representation is invariant for high and low rewards and if so, how this context-dependent adaptation process is implemented. The results showed that the prediction error coding in the striatum is invariant across different reward magnitudes, whereas this invariance is achieved by a context-dependent modulation of striatal coupling with other reward sensitive brain regions, namely the MPFC and the midbrain (Park et al., revised manuscript).

## 3.1 Value impacts valuation

Most decision options have both positive (benefit) and negative (cost) aspects. To facilitate decisions we need to integrate these values and build an overall subjective value of an option (Kable and Glimcher, 2007). One possible integration mechanism is context-independent valuation; i.e. a simple weighted sum of different values. In contrast, an

interactive integration mechanism, where valuation of the different aspects depends on the value of the other aspects, accounts for the context dependency.

I developed a decision task, in which subjects could accept or reject a choice option in each trial. The choice options incorporated two attributes that were of positive and negative value and of different nature; physical pain (electric shock) and monetary gain. The monetary amount and the pain level varied pseudo-randomly in each trial and when the offer was accepted, the subject received both money and pain, whereas when rejected, neither was given (FIGURE 3A). Two sets of models were tested. The independent models assume that the subjective value of an option results from a weighted sum of money and pain:

$$SV(x) = \beta_{\text{pain}}\, p_x + \beta_{\text{money}} m_x \quad (1)$$

Whereas the interactive models assume an additional parameter accounting for the interaction of the two:

$$SV(x) = \beta_{\text{pain}}\, p_x + \beta_{\text{money}} m_x + \beta_{\text{pain x money}}\, p_x m_x \quad (2)$$

Here, *SV* is the subjective value of the option, $p_x$ is the pain level, $m_x$ is monetary gain of the option, the *βs* represent the weight for pain, money and their interaction, respectively. For completeness, we modelled both mechanisms with linear and non-linear value functions, resulting in four models (FIGURE 3C).

The first step was to compare the models on the behavioural data. Here, the interactive models made better predictions when comparing models with linear value functions. However, with nonlinear value functions, the models were equally good (FIGURE 3B). Hence, the behavioural data could not provide decisive information about which integration model is more likely to be correct. The application of the models to imaging data showed a similar correlation pattern with BOLD responses for all four models (FIGURE 3C).

Here, the outputs of all four models, that is, the subjective values of the option were represented in the MPFC/OFC. The MPFC/OFC has been previously shown to encode value signals (Philiastides et al., 2010;Rangel and Hare, 2010;O'Doherty, 2007;Kahnt et al., 2010). A statistical model comparison on the imaging data, however, revealed that BOLD responses in the SGACC could be significantly better predicted by the interactive models (FIGURE 4A). This superiority was present for both linear and non-linear value functions, indicating that the imaging data is able to provide decisive information about the superiority of the interactive model (FIGURE 4B). Finally, a psycho-physiological interaction analysis was performed with the SGACC as a seed region and different levels of money and pain as psychological variables. This analysis revealed that the SGACC modulates its connectivity with the amygdala as a function of the pain-by-money interaction (FIGURE 4C). Specifically, the connectivity was modulated by money only under the high pain condition, whereas under the low pain condition, the modulation was not present (FIGURE 4D). This PPI result demonstrates that the value interaction relies on a dynamic modulation of the SGACC-amygdala coupling.

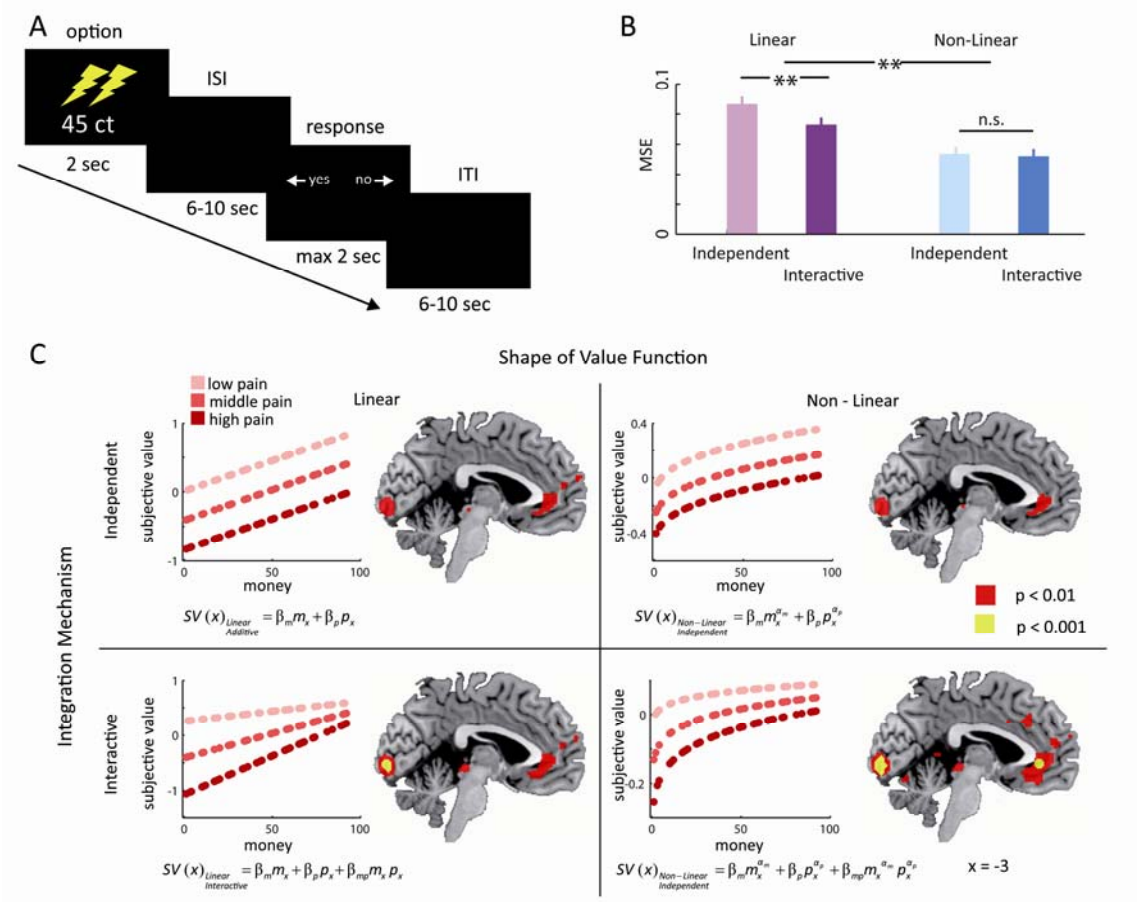


**FIGURE 3** Subjective value computation based on four different integration models

**A.** Task design. In each trial, subjects could either accept or reject a choice option that was a combination of physical pain and monetary gain. **B.** MSE (mean squared error) of the four models in predicting choice behaviour. When value functions were modelled linearly, interactive model made less errors compared to the independent models, however, with non-linear value functions, both models performed equally well. Error bars indicate s.e.m. **C.** On the left side of each panel, the subjective values of each model are depicted. Note that in interactive models (lower row), the subjective values from different pain levels are not only shifted on the y axis, but also have different slopes; i.e. the increase in monetary value is modulated by the combined pain level (data from a single subject for demonstration). The right side of panel shows brain regions encoding the subjective value of the four models (group data, sagittal view).

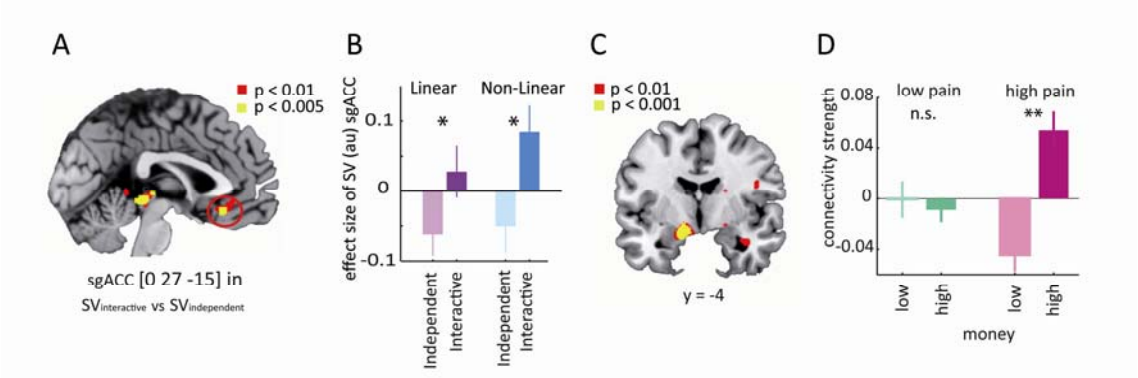


**FIGURE 4** Model comparisons on FMRI data and connectivity analysis

**A.** The comparison of the models on neural data revealed that SGACC activity is significantly better predicted by the interactive compared to the independent integration mechanism (collapsed over value functions). **B.** This result was still significant when testing within each value function separately. **C.** The PPI analysis with the SGACC as seed region and the money-by-pain interaction as psychological variable revealed significant modulation of SGACC-amygdala connectivity. **D.** Mean corrected connectivity strength between the amygdala and the SGACC. Functional connectivity between the SGACC and the left amygdala is enhanced when comparing high and low monetary offers in the context of high pain. Importantly, this connectivity modulation is absent in the low pain condition. Error bars indicate s.e.m.

### 3.2 Adaptive coding of reward prediction errors

The second project investigates the context-dependent coding of prediction errors in the human brain. PEs have been shown to be invariant across different reward magnitudes and this is only possible with a magnitude dependent normalization process. Hence, the context here is reward magnitudes and the modulation refers to the normalization of different reward magnitudes that enables adaptive coding of PE. Subjects were asked to perform a simple reward prediction task with different reward magnitudes (FIGURE 5A). In each trial, they first saw a reward-predicting cue. After a delay, the reward was delivered or omitted depending on the cued probability. Importantly, we had four different cues; high and low magnitude (1€ and 10cent, respectively) combined with high and low probability (66% and 33%, respectively).

The first analysis aimed to test whether the striatal PE was adaptively coded, focusing on the time point of reward outcome. By comparing the correlation between PE and striatal BOLD signal across the two magnitudes, we confirmed the indifference in PE coding; i.e. context-dependent adaptation (FIGURE 5B & 5C). Furthermore, an explicit comparison of context-dependent PE and context-independent PE showed that the context-dependent PE could significantly better predict the striatal BOLD response (FIGURE 5D). In a next step, to investigate how this context-dependent normalization is implemented, an effective connectivity analysis was performed, with the striatum as seed region. Here, the psychological variable was the different reward contexts. This analysis revealed significant context-dependent modulation of effective connectivity between the striatum and the MPFC /midbrain (FIGURE 5E). Importantly, in high reward conditions, there was less connectivity compared to the low reward condition (FIGURE 5F).

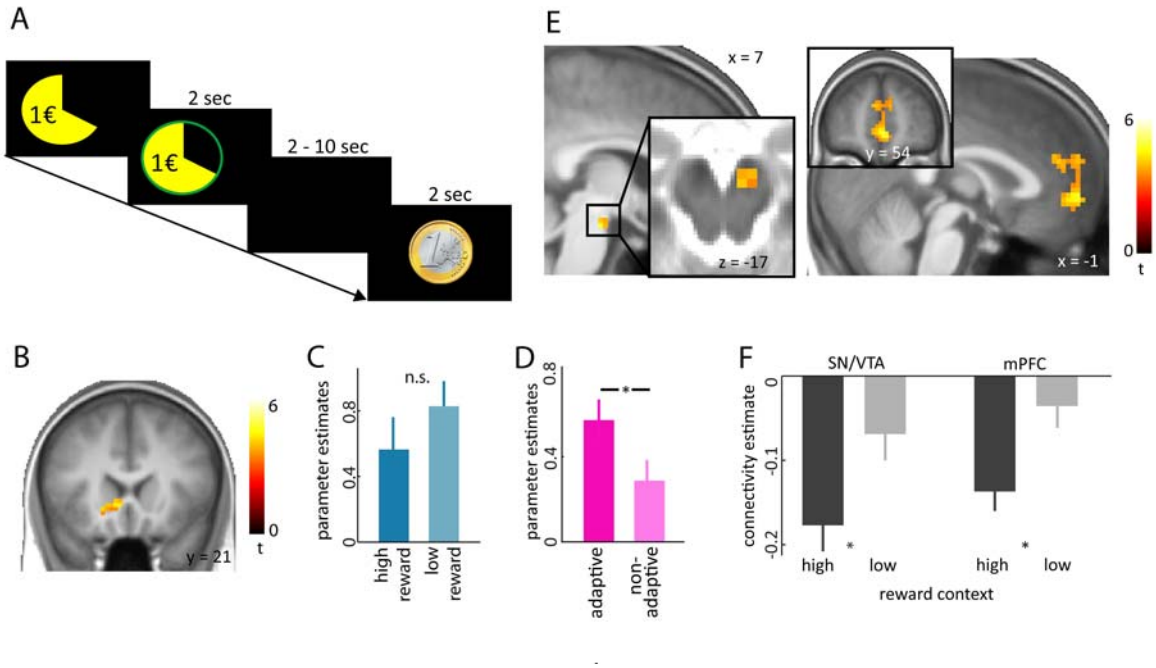


**FIGURE 5** Adaptive coding of reward prediction errors is gated by striatal connectivity

**A.** Task design. In each trial, a reward-predicting cue was presented, after which subjects were asked to press a button. After a variable delay, the reward outcome was shown. **B.** Striatal BOLD responses showed a significant correlation with reward prediction errors. **C.** Importantly, this prediction error was indifferent for high and low rewards, confirming adaptive coding of prediction errors in the striatum. **D. T**he adaptive PE (modulated only by probability) could predict the striatal BOLD significantly better compared to the non-adaptive PE (product of magnitude and probability). **E.** PPI analysis with striatal seed region revealed that striatal connectivity with MPFC and midbrain was significantly modulated by reward magnitudes. **F.** Specifically, the striatal coupling was significantly lower during high compared to low reward, indicating down-regulation of striatal activity during high reward outcomes to implement adaptation of prediction errors. All error bars indicate s.e.m.

# 4. Conclusions and future directions

In the previous chapter, I have presented the results of two studies investigating context-dependent modulation of value processing. Here I will first discuss the results of the two projects. The second part proposes a neurobiological model for value processing in a broader frame. Finally, the third part suggests how the proposed model of value processing can be tested in future experiments.

The results presented in this thesis demonstrate how reward processing flexibly adapts to a given context. Why is this important? What is the benefit of this mechanism? One possible answer is that this mechanism facilitates behavioural adaptation. The results of the first project show that reward valuation is interactively modified in the context of negative values. An interactive process changes the valuation of the positive reward depending on the negative value, thus facilitating optimal behaviour to maximize reward and minimize punishment (Fields, 2007;Dum and Herz, 1984). E.g. in face of great danger, it is beneficial to ignore the combined small benefit and to avoid the option. Accordingly, interactive value integration downscales the positive reward value, assigning less value to it than it would be the case without the negative value. In this case, the subjective value created by the interactive model is smaller than that of the additive model. This may serve to reduce the conflict of approach and avoidance behaviour and facilitate decision making.

However, such a beneficial mechanism can also produce irrational behaviours such as intransitivity. Transitivity postulates, that in case an apple is preferred over an orange, and an orange over a pineapple, the apple should also be preferred over the pineapple. Choices need to be transitive, because one option cannot be better and worse than another option at the same time (von Neumann and Morgenstern, 1944;Samuelson, 1938). However, humans and animals often violate transitivity (Tversky, 1969;Shafir, 1994). Specifically,

intransitive choices are revealed when individuals choose between outcomes that vary along several aspects, such as different values (Tversky, 1969). The interactive value integration mechanism is able to predict such intransitive choice behaviour, because this model predicts that the valuation of one and the same reward changes depending on the cost associated with it. Furthermore, a recent FMRI study investigating intransitivity demonstrates that activity in the SGACC correlates with context-dependent desirability, a variable that accounts for intransitivity (Kalenscher et al., 2010) in line with the presented result of the thesis (Park et al., 2011).

The results of the second experiment show that the PE representation adapts depending on reward magnitudes (Park et al. revised manuscript). This adaptive coding of PE enables us to remain sensitive across a large range of rewards. In case this PE computation is context-independent, we could not learn from small rewards. In other words, in all situations, only the prediction errors of extremely high rewards would be behaviourally relevant and prediction errors of small rewards would never impact behaviour.

This context-dependent normalization is accompanied by a change in the connectivity between the striatum and the MPFC/midbrain. Studies investigating the dynamics of neuronal activation in this anatomical network support our connectivity finding. These studies indicate that activation of the PFC regulates striatal dopamine release via inhibitory midbrain neurons (Haber and McFarland, 1999;Haber et al., 1995;Haber and Knutson, 2010). Specifically, PFC neurons activate midbrain GABAergic cells that in turn inhibit neighbouring dopaminergic neurons projecting to the striatum (Karreman and Moghaddam, 1996;Sesack and Pickel, 1992;Sesack et al., 1989;Frankle et al., 2006).

Taken together, the results of both experiments lead to a broader picture of how the brain can flexibly process values in different contexts. Based on these results, the following

model can be proposed (FIGURE 6). Changes in SGACC-amygdala coupling modulate the value of the reward depending on the cost associated with it. The output of this computation, the subjective value, is represented in the MPFC/OFC. Evidence from previous studies points toward a role of MPFC/OFC as working memory for expected rewards (Schoenbaum et al., 1998;Wallis, 2007). Specifically, a recent study has shown that when a reward predicting cue is presented, the activity pattern in the MPFC/OFC mimics the pattern of reward receipt (Kahnt et al., 2010;Kahnt et al., 2011). Furthermore, it has been suggested that this expected value representation in the MPFC/OFC is updated by means of PE signals from the midbrain (VTA) (Schoenbaum et al., 2009;Takahashi et al., 2009;Takahashi et al., 2011). Hence, it can be assumed that the MPFC/OFC bridges the delay between the reward cue and the outcome by maintaining expected outcome representations. At the time of the reward outcome, this representation of expected reward enables the MPFC/OFC in concert with the midbrain to regulate activity in the striatum to adjust the prediction error depending on the expected magnitude of reward. Prediction errors in turn, change the expected value of cues in the OFC and thus future behaviour. All these regions have different roles in processing specific aspects of reward. However, these different regions do not work in isolation but are linked together by means of changes in functional connectivity. Thus, this network allows the representation of all aspects of reward and, because it represents value in a context-dependent fashion, remains sensitive to small differences in value at the same time.

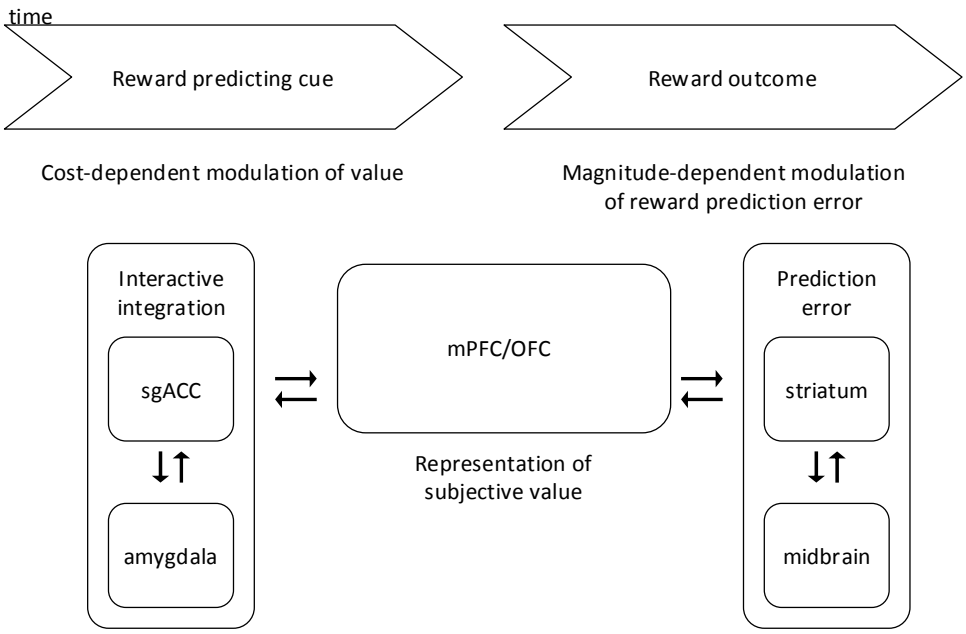


**FIGURE 6** A potential mechanism of context-dependent value processing

When encountering a reward predicting cue with cost and benefit aspects, SGACC and amygdala modulate the reward value depending on its cost. The output of this computation, namely the subjective value is subsequently represented in the MPFC/OFC and is used to guide choice behaviour. Furthermore, the MPFC/OFC sustains the subjective value information until the predicted reward outcome occurs. The maintained information is then used to regulate the striatal PE to enable adaptive coding. This context-dependent modulation is implemented by changes in functional connectivity between regions (represented by small arrows).

This model suggests several questions to be tested. First, people tend to seek immediate rewards and delayed pay (Weber et al., 2004;Weber and Johnson, 2006). This asymmetric discounting (Loewenstein, 1988) is typically explained by loss aversion as formalized by prospect theory (Kahneman and Tversky, 1979). Hence, people prefer an

option in which the reward value is presented first, then its cost, compared to an option with the opposite sequence, even if those options are objectively the same. The model based on the results presented in this thesis would predict that the sequence-dependent modulation also relies on the SGACC-amygdala network. Specifically, depending on the sequence, it is likely that the modulation is stronger in the reward-cost compared to the cost-reward sequence. Furthermore, it could be tested, whether individual differences in loss-aversion are reflected in SGACC-amygdala coupling.

Second, this model can be tested in addicted patients, such as substance dependence or gambling. For these patients, the reward value of the drug is so powerful, triggering strong drug seeking behaviour, whereas all the other potential rewards seem be behaviourally irrelevant (Kalivas and Volkow, 2005;Nesse and Berridge, 1997). Recently, it has been shown that the prediction error coding itself is not impaired in alcohol-dependent patients (Park et al., 2010). However, in the frame of our model, it can be hypothesized, that these patients have an impaired context-dependent adaptation, such that their behaviour is only influenced by the substance related PE signal.

Third, it is an open question, whether context-dependent adaptation of value processing is also applied in the social domain. Theory-of-mind, the ability to understand other's mental state has been associated with distinct brain regions, such as dorsomedial prefrontal cortex (DMPFC), temporo-parietal junction (TPJ) and superior temporal sulcus (STS) (Behrens et al., 2009). It is possible that these regions interact with the network of the suggested model. Hence, future studies could investigate 1) whether there is active context-dependent reward processing for another person in the same manner and 2) whether this also relies on the same brain network.

In conclusion, the results of this dissertation considerably advance our knowledge about the neurobiology of context-dependent value modulation in humans. Using sophisticated FMRI analysis methods, they show that reward value is flexibly adapted to its context, and that reward prediction error computation adapts to different reward magnitudes. Furthermore, they shed light onto its underlying neural mechanism. Finally, these findings and the model derived from them raise new questions for future research.

# 5. Reference List

Aharon I, Etcoff N, Ariely D, Chabris CF, O'Connor E, Breiter HC (2001) Beautiful faces have variable reward value: fMRI and behavioral evidence. Neuron 32:537-551.

Behrens TE, Hunt LT, Rushworth MF (2009) The computation of social behavior. Science 324:1160-1164.

Bhatt MA, Lohrenz T, Camerer CF, Montague PR (2010) Neural signatures of strategic types in a two-person bargaining game. Proc Natl Acad Sci U S A 107:19720-19725.

Bingel U, Lorenz J, Schoell E, Weiller C, Buchel C (2006) Mechanisms of placebo analgesia: rACC recruitment of a subcortical antinociceptive network. Pain 120:8-15.

Blood AJ, Zatorre RJ, Bermudez P, Evans AC (1999) Emotional responses to pleasant and unpleasant music correlate with activity in paralimbic brain regions. Nat Neurosci 2:382-387.

Breiter HC, Aharon I, Kahneman D, Dale A, Shizgal P (2001) Functional imaging of neural responses to expectancy and experience of monetary gains and losses. Neuron 30:619-639.

Bruni L, Sugden R (2007) The road not taken: how psychology was removed from economics, and how it might be brought back. Economic Journal 117:146-173.

Camara E, Rodriguez-Fornells A, Munte TF (2008) Functional connectivity of reward processing in the brain. Front Hum Neurosci 2:19.

Chib VS, Rangel A, Shimojo S, O'Doherty JP (2009) Evidence for a common representation of decision values for dissimilar goods in human ventromedial prefrontal cortex. J Neurosci 29:12315-12320.

Dum J, Herz A (1984) Endorphinergic modulation of neural reward systems indicated by behavioral changes. Pharmacol Biochem Behav 21:259-266.

Dunn FA, Lankheet MJ, Rieke F (2007) Light adaptation in cone vision involves switching between receptor and post-receptor sites. Nature 449:603-606.

Elliott R, Newman JL, Longe OA, Deakin JFW (2003) Differential response patterns in the striatum and orbitofrontal cortex to financial reward in humans: a parametric functional magnetic resonance imaging study. J Neurosci 23:303-307.

Fields HL (2007) Understanding how opioids contribute to reward and analgesia. Reg Anesth Pain Med 32:242-246.

Fox MD, Zhang D, Snyder AZ, Raichle ME (2009) The global signal and observed anticorrelated resting state brain networks. J Neurophysiol 101:3270-3283.

Francis S, Rolls ET, Bowtell R, McGlone F, O'Doherty J, Browning A, Clare S, Smith E (1999) The representation of pleasant touch in the brain and its relationship with taste and olfactory areas. Neuroreport 10:453-459.

Frank MJ, Claus ED (2006) Anatomy of a decision: striato-orbitofrontal interactions in reinforcement learning, decision making, and reversal. Psychol Rev 113:300-326.

Frankle WG, Laruelle M, Haber SN (2006) Prefrontal cortical projections to the midbrain in primates: evidence for a sparse connection. Neuropsychopharmacology 31:1627-1636.

Friston KJ, Buechel C, Fink GR, Morris J, Rolls E, Dolan RJ (1997) Psychophysiological and modulatory interactions in neuroimaging. Neuroimage 6:218-229.

Fujiwara J, Tobler PN, Taira M, Iijima T, Tsutsui K (2009) Segregated and integrated coding of reward and punishment in the cingulate cortex. J Neurophysiol 101:3284-3293.

Gitelman DR, Penny WD, Ashburner J, Friston KJ (2003) Modeling regional and psychophysiologic interactions in fMRI: the importance of hemodynamic deconvolution. Neuroimage 19:200-207.

Glimcher PW, Rustichini A (2004) Neuroeconomics: the consilience of brain and decision. Science 306:447-452.

Haber SN, Fudge JL, McFarland NR (2000) Striatonigrostriatal pathways in primates form an ascending spiral from the shell to the dorsolateral striatum. J Neurosci 20:2369-2382.

Haber SN, Knutson B (2010) The reward circuit: linking primate anatomy and human imaging. Neuropsychopharmacology 35:4-26.

Haber SN, Kunishio K, Mizobuchi M, Lynd-Balta E (1995) The orbital and medial prefrontal circuit through the primate basal ganglia. J Neurosci 15:4851-4867.

Haber SN, McFarland NR (1999) The concept of the ventral striatum in nonhuman primates. Ann N Y Acad Sci 877:33-48.

Hampton AN, Bossaerts P, O'Doherty JP (2008) Neural correlates of mentalizing-related computations during strategic interactions in humans. Proc Natl Acad Sci U S A 105:6741-6746.

Hampton AN, Bossaerts P, O'Doherty JP (2006) The role of the ventromedial prefrontal cortex in abstract state-based inference during decision making in humans. J Neurosci 26:8360-8367.

Handwerker DA, Ollinger JM, D'esposito M (2004) Variation of BOLD hemodynamic responses across subjects and brain regions and their effects on statistical analyses. Neuroimage 21:1639-1651.

Huber GP (1974) Multi-attribute utility models: A review of field and field-like studies. Manage Sci 20:1393-1402.

Jungermann H (1976) Rationale Entscheidungen. Bern: Verlag Hans Huber Bern.

Kable JW, Glimcher PW (2007) The neural correlates of subjective value during intertemporal choice. Nat Neurosci 10:1625-1633.

Kahneman D, Tversky A (1979) Prospect Theory - Analysis of Decision Under Risk. Econometrica 47:263-291.

Kahnt T, Heinzle J, Park SQ, Haynes JD (2010) The neural code of reward anticipation in human orbitofrontal cortex. Proc Natl Acad Sci U S A 107:6010-6015.

Kahnt T, Heinzle J, Park SQ, Haynes JD (2011) Decoding different roles for vmPFC and dlPFC in multi-attribute decision making. Neuroimage 56:709-715.

Kahnt T, Park SQ, Cohen MX, Beck A, Heinz A, Wrase J (2009) Dorsal Striatal-midbrain Connectivity in Humans Predicts How Reinforcements Are Used to Guide Decisions. J Cogn Neurosci.

Kalenscher T, Tobler PN, Huijbers W, Daselaar SM, Pennartz CM (2010) Neural signatures of intransitive preferences. Front Hum Neurosci 4.

Kalivas PW, Volkow ND (2005) The neural basis of addiction: A pathology of motivation and choice. Am J Psychiatry 162:1403-1413.

Karreman M, Moghaddam B (1996) The prefrontal cortex regulates the basal release of dopamine in the limbic striatum: an effect mediated by ventral tegmental area. J Neurochem 66:589-598.

Keeney R, Raiffa H (1976) Decisions with multiple objectives: preferences and value tradeoffs. New York: Wiley.

Kim H, Shimojo S, O'Doherty JP (2011) Overlapping responses for the expectation of juice and money rewards in human ventromedial prefrontal cortex. Cereb Cortex 21:769-776.

Knutson B, Adams CM, Fong GW, Hommer D (2001a) Anticipation of increasing monetary reward selectively recruits nucleus accumbens. J Neurosci 21:RC159.

Knutson B, Fong GW, Adams CM, Varner JL, Hommer D (2001b) Dissociation of reward anticipation and outcome with event-related fMRI. Neuroreport 12:3683-3687.

Kobayashi S, Pinto de CO, Schultz W (2010) Adaptation of reward sensitivity in orbitofrontal neurons. J Neurosci 30:534-544.

Kringelbach ML, O'Doherty J, Rolls ET, Andrews C (2003) Activation of the human orbitofrontal cortex to a liquid food stimulus is correlated with its subjective pleasantness. Cereb Cortex 13:1064-1071.

Levy DJ, Glimcher PW (2011) Comparing apples and oranges: using reward-specific and reward-general subjective value representation in the brain. J Neurosci 31:14693-14707.

Loewenstein G (1988) Frames of mind in intertemporal choice. Manage Sci 34:200-214.

Loewenstein G, Rick S, Cohen JD (2008) Neuroeconomics. Annu Rev Psychol 59:647-672.

Lohrenz T, McCabe K, Camerer CF, Montague PR (2007) Neural signature of fictive learning signals in a sequential investment task. Proc Natl Acad Sci U S A 104:9493-9498.

Louie K, Grattan LE, Glimcher PW (2011) Reward value-based gain control: divisive normalization in parietal cortex. J Neurosci 31:10627-10639.

Mazur JE, Biondi DR (2009) Delay-amount tradeoffs in choices by pigeons and rats: hyperbolic versus exponential discounting. J Exp Anal Behav 91:197-211.

Mohr PN, Biele G, Krugel LK, Li SC, Heekeren HR (2010) Neural foundations of risk-return trade-off in investment decisions. Neuroimage 49:2556-2563.

Montague PR, Berns GS (2002) Neural economics and the biological substrates of valuation. Neuron 36:265-284.

Murphy K, Birn RM, Handwerker DA, Jones TB, Bandettini PA (2009) The impact of global signal regression on resting state correlations: are anti-correlated networks introduced? Neuroimage 44:893-905.

Navalpakkam V, Koch C, Rangel A, Perona P (2010) Optimal reward harvesting in complex perceptual environments. Proc Natl Acad Sci U S A 107:5232-5237.

Nesse RM, Berridge KC (1997) Psychoactive drug use in evolutionary perspective. Science 278:63-66.

Nieuwenhuis S, Heslenfeld DJ, von Geusau NJ, Mars RB, Holroyd CB, Yeung N (2005) Activity in human reward-sensitive brain areas is strongly context dependent. Neuroimage 25:1302-1309.

O'Doherty JP (2007) Lights, Camembert, Action! The role of human orbitofrontal cortex in encoding stimuli, rewards and choices. Ann N Y Acad Sci.

O'Doherty JP, Buchanan TW, Seymour B, Dolan RJ (2006) Predictive neural coding of reward preference involves dissociable responses in human ventral midbrain and ventral striatum. Neuron 49:157-166.

O'Doherty JP, Deichmann R, Critchley HD, Dolan RJ (2002) Neural responses during anticipation of a primary taste reward. Neuron 33:815-826.

O'Doherty JP, Hampton A, Kim H (2007) Model-based FMRI and its application to reward learning and decision making. Ann N Y Acad Sci 1104:35-53.

O'Doherty JP, Kringelbach ML, Rolls ET, Hornak J, Andrews C (2001) Abstract reward and punishment representations in the human orbitofrontal cortex. Nat Neurosci 4:95-102.

Padoa-Schioppa C (2009) Range-adapting representation of economic value in the orbitofrontal cortex. J Neurosci 29:14004-14014.

Padoa-Schioppa C, Assad JA (2008) The representation of economic value in the orbitofrontal cortex is invariant for changes of menu. Nat Neurosci 11:95-102.

Park SQ, Kahnt T, Beck A, Cohen MX, Dolan RJ, Wrase J, Heinz A (2010) Prefrontal cortex fails to learn from reward prediction errors in alcohol dependence. J Neurosci 30:7749-7753.

Park SQ, Kahnt T, Rieskamp J, Heekeren HR (2011) Neurobiology of value integration: when value impacts valuation. J Neurosci 31:9307-9314.

Park SQ, Kahnt T, Talmi D, Rieskamp J, Dolan RJ, Heekeren HR Adaptive coding of reward prediction errors is gated by striatal coupling. Proc Natl Acad Sci U S A revised manuscript.

Pavlow P (1927) Conditioned Reflexes. London: Oxford Univ. Press.

Pessiglione M, Seymour B, Flandin G, Dolan RJ, Frith CD (2006) Dopamine-dependent prediction errors underpin reward-seeking behaviour in humans. Nature 442:1042-1045.

Pessoa L, McKenna M, Gutierrez E, Ungerleider LG (2002) Neural processing of emotional faces requires attention. Proc Natl Acad Sci U S A 99:11458-11463.

Peters J, Buchel C (2010) Neural representations of subjective reward value. Behav Brain Res 213:135-141.

Phelps EA, Delgado MR, Nearing KI, LeDoux JE (2004) Extinction learning in humans: role of the amygdala and vmPFC. Neuron 43:897-905.

Philiastides MG, Biele G, Heekeren HR (2010) A mechanistic account of value computation in the human brain. Proc Natl Acad Sci U S A 107:9430-9435.

Rangel A, Camerer C, Montague PR (2008) A framework for studying the neurobiology of value-based decision making. Nat Rev Neurosci 9:545-556.

Rangel A, Hare T (2010) Neural computations associated with goal-directed choice. Curr Opin Neurobiol 20:262-270.

Rescorla RA & Wagner AR (1972) A theory of Pavlovian conditioning: variations in the effectiveness of reinforcement and nonreinforcement. In: Classical Conditioning II: Current Research and Theory, eds Black AH, Prokasy WF, (Appleton Century Crofts, New York), pp 64 – 99.

Samuelson PA (1938) A note on the pure theory of consumer's behavior. Econometrica 5:353-354.

Schoenbaum G, Chiba AA, Gallagher M (1998) Orbitofrontal cortex and basolateral amygdala encode expected outcomes during learning. Nat Neurosci 1:155-159.

Schoenbaum G, Roesch MR, Stalnaker TA, Takahashi YK (2009) A new perspective on the role of the orbitofrontal cortex in adaptive behaviour. Nat Rev Neurosci 10:885-892.

Schultz W, Dayan P, Montague PR (1997) A neural substrate of prediction and reward. Science 275:1593-1599.

Sesack SR, Deutch AY, Roth RH, Bunney BS (1989) Topographical organization of the efferent projections of the medial prefrontal cortex in the rat: an anterograde tract-tracing study with Phaseolus vulgaris leucoagglutinin. J Comp Neurol 290:213-242.

Sesack SR, Pickel VM (1992) Prefrontal cortical efferents in the rat synapse on unlabeled neuronal targets of catecholamine terminals in the nucleus accumbens septi and on dopamine neurons in the ventral tegmental area. J Comp Neurol 320:145-160.

Sescousse G, Redoute J, Dreher JC (2010) The architecture of reward value coding in the human orbitofrontal cortex. J Neurosci 30:13095-13104.

Seymour B, O'Doherty JP, Koltzenburg M, Wiech K, Frackowiak R, Friston K, Dolan R (2005) Opponent appetitive-aversive neural processes underlie predictive learning of pain relief. Nat Neurosci 8:1234-1240.

Shafir S (1994) Intransitivity of preferences in honey bees: support for 'comparative' evaluation of foraging options. Anim Behav 48:55-67.

Skinner B (1953) Science and Human Behavior. New York: Free Press.

Skinner B (1938) The Behavior of Organisms. New York: Appleton-Century-Crofts.

Smith DV, Hayden BY, Truong TK, Song AW, Platt ML, Huettel SA (2010) Distinct value signals in anterior and posterior ventromedial prefrontal cortex. J Neurosci 30:2490-2495.

Stone M (1974) Cross-validatory choice and assessment of statistical predictions. J R Statist Soc Series B Stat Methodol 36:111-147.

Sutton R, Barto A (1998) Reinforcement Learning: An Introduction. Cambridge, MA: MIT Press.

Takahashi YK, Roesch MR, Stalnaker TA, Haney RZ, Calu DJ, Taylor AR, Burke KA, Schoenbaum G (2009) The orbitofrontal cortex and ventral tegmental area are necessary for learning from unexpected outcomes. Neuron 62:269-280.

Takahashi YK, Roesch MR, Wilson RC, Toreson K, O'Donnell P, Niv Y, Schoenbaum G (2011) Expectancy-related changes in firing of dopamine neurons depend on orbitofrontal cortex. Nat Neurosci 14:1590-1597.

Thorndike E (1911) Animal Intelligence: Experimental Studies. New York: MacMillan.

Tobler PN, Fiorillo CD, Schultz W (2005) Adaptive coding of reward value by dopamine neurons. Science 307:1642-1645.

Tremblay L, Schultz W (1999) Relative reward preference in primate orbitofrontal cortex. Nature 398:704-708.

Tversky A (1969) Intransitivity of preferences. Psychol Rev 76:31-48.

Van Dijk KR, Hedden T, Venkataraman A, Evans KC, Lazar SW, Buckner RL (2010) Intrinsic functional connectivity as a tool for human connectomics: theory, properties, and optimization. J Neurophysiol 103:297-321.

von Helversen B., Rieskamp J (2009) Models of quantitative estimations: rule-based and exemplar-based processes compared. J Exp Psychol Learn Mem Cogn 35:867-889.

von Neumann J, Morgenstern O (1944) Theory of Games and Economic Behavior. Princeton, NJ: University Press.

Wager TD, Matre D, Casey KL (2006) Placebo effects in laser-evoked pain potentials. Brain Behav Immun 20:219-230.

Wallenius J, Dyer JS, Fishburn PC, Steuer RE, Zionts S, Deb K (2008) Multiple criteria decision making, multiattribute utility theory: recent accomplishments and what lies ahead. Manage Sci 54:1336-1349.

Wallis JD (2007) Orbitofrontal cortex and its contribution to decision-making. Annu Rev Neurosci 30:31-56.

Weber EU, Johnson EJ (2006) Constructing preferences from memories. In: The construction of preference (Lichtenstein S, Slovic P, eds), pp 397-410. New York: Cambridge University Press.

Weber EU, Shafir S, Blais AR (2004) Predicting risk sensitivity in humans and lower animals: risk as variance or coefficient of variation. Psychol Rev 111:430-445.

Wiech K, Ploner M, Tracey I (2008) Neurocognitive aspects of pain perception. Trends Cogn Sci 12:306-313.

# Supplements

## A Eidesstattliche Erklärung

Hiermit erkläre ich an Eides statt,

dass ich die vorliegende Arbeit selbstständig und ohne unerlaubte Hilfe verfasst habe,

dass ich mich nicht bereits anderwärts um einen Doktorgrad beworben habe und keinen Doktorgrad in dem Promotionsfach Psychologie besitze und

dass ich die zugrunde liegende Promotionsordnung vom 02.12.2008 kenne.

Berlin, den 05.12.2011 So Young Park

## B Research articles

**Project I**

Park, S.Q., Kahnt, T., Rieskamp, J., Heekeren, H.R. (2011).

Neurobiology of value integration: When value impacts valuation.

*J Neurosci*, 31(25): 9307-9314

doi: 10.1523/JNEUROSCI.4973-10.2011

Behavioral/Systems/Cognitive

# Neurobiology of Value Integration: When Value Impacts Valuation

**Soyoung Q Park,**[1,2,3] **Thorsten Kahnt,**[3,4] **Jörg Rieskamp,**[5] **and Hauke R. Heekeren**[1,2,3]

[1]Department of Education and Psychology, Freie Universität Berlin, 14195 Berlin, Germany, [2]Neurocognition of Decision Making Group, Max Planck Institute for Human Development, 14195 Berlin, Germany, [3]Berlin School of Mind and Brain, Humboldt Universität zu Berlin, 10117 Berlin, Germany, [4]Bernstein Center for Computational Neuroscience, Charité–Universitätsmedizin Berlin, 10117 Berlin, Germany, and [5]Department of Psychology, University of Basel, 4051 Basel, Switzerland

**Everyday choice options have advantages (positive values) and disadvantages (negative values) that need to be integrated into an overall subjective value. For decades, economic models have assumed that when a person evaluates a choice option, different values contribute independently to the overall subjective value of the option. However, human choice behavior often violates this assumption, suggesting interactions between values. To investigate how qualitatively different advantages and disadvantages are integrated into an overall subjective value, we measured the brain activity of human subjects using fMRI while they were accepting or rejecting choice options that were combinations of monetary reward and physical pain. We compared different subjective value models on behavioral and neural data. These models all made similar predictions of choice behavior, suggesting that behavioral data alone are not sufficient to uncover the underlying integration mechanism. Strikingly, a direct model comparison on brain data decisively demonstrated that interactive value integration (where values interact and affect overall valuation) predicts neural activity in value-sensitive brain regions significantly better than the independent mechanism. Furthermore, effective connectivity analyses revealed that value-dependent changes in valuation are associated with modulations in subgenual anterior cingulate cortex–amygdala coupling. These results provide novel insights into the neurobiological underpinnings of human decision making involving the integration of different values.**

## Introduction

In everyday life, we choose between options with multiple attributes. The attributes of an option (e.g., shoes) can be qualitatively different (aesthetics and expenses) and are associated with positive or negative values. For successful choice behavior, individuals need to integrate the different values into an overall subjective value.

Behavioral economics has investigated value integration mechanisms to predict choice behavior across a distribution of positive and negative values. Multiattribute utility theory suggests that the subjective value of multiattribute options equals the attributes' weighted sum (Keeney and Raiffa, 1976; Wallenius et al., 2008). Although these models can predict choice behavior well (Huber, 1974; Wallenius et al., 2008), they require that the preference order of one attribute is independent of other attributes. However, human choice often violates this (Keeney and Raiffa, 1976); for example, when selecting a dinner menu with cheese, red wine has a higher value than white wine. But, with fish, white wine has a higher value. Here, an independent model fails to predict choice, whereas an interactive integration model would successfully predict choice by permitting an extra term for the dependence of attributes.

How the neural systems mediate the value integration is not well understood. The subgenual anterior cingulate cortex (sgACC) has been shown to encode both positive and negative values (Blood et al., 1999; Plassmann et al., 2010). Also, the amygdala represents values independent of valence (Breiter et al., 1996, 2001; Becerra et al., 2001; Gasic et al., 2009). Furthermore, these structures play a key role in both affect (Phelps et al., 2004) and pain regulation (Bingel et al., 2006; Wiech et al., 2008). Thus, the sgACC and the amygdala are ideally suited to facilitate interactive value integration.

In this study, we investigated how the brain integrates values across discrete stimuli into one subjective value to guide decision making. We hypothesized that (1) different values affect each other and (2) the sgACC and amygdala are critically involved. To test these hypotheses, we measured brain activity using fMRI while subjects accepted or rejected offers that were combinations of qualitatively different values of different valence (pain and money). The combination of values included a parametric variation in their intensities.

A well established approach to investigate cognitive processes underlying decision making is to compare cognitive models on behavioral data (O'Doherty et al., 2007; Mazur and Biondi, 2009; Talmi et al., 2009; Bhatt et al., 2010; Navalpakkam et al., 2010). However, if competing models predict the same pattern of choices, behavioral data are limited (Bruni and Sugden, 2007). In these cases, forcing the models to predict neural activity can provide decisive evidence (Glimcher and Rustichini, 2004; Hampton

Received Sept. 21, 2010; revised March 24, 2011; accepted May 4, 2011.

Author contributions: S.Q.P., T.K., J.R., and H.R.H. designed research; S.Q.P. performed research; S.Q.P. and T.K. analyzed data; S.Q.P., T.K., J.R., and H.R.H. wrote the paper.

This work was supported by the Excellence Initiative of the German Federal Ministry of Education and Research (DFG Grants GSC86/1-2009 and EXC 302), the Max Planck Society, and the Swiss National Science Foundation (SNF 100014_130352).

Correspondence should be addressed to Soyoung Q. Park, Psychology of Emotion/Affective Neuroscience, Department of Education and Psychology, Freie Universität Berlin, Habelschwerdter Allee 45, 14195 Berlin, Germany. E-mail: Soyoung.q.park@gmail.com.

DOI:10.1523/JNEUROSCI.4973-10.2011

 0270-6474/11/319307-08$15.00/0

et al., 2006, 2008; Sanfey et al., 2006; Kable and Glimcher, 2007; Loewenstein et al., 2008). We tested four different subjective value models with either independent or interactive value integration mechanisms. We applied these models directly on behavioral and neural data, looking for decisive information about the implemented mechanism in the brain. Finally, we investigated how different brain regions interact when one attribute's value affects another valuation process.

## Materials and Methods

### *Subjects*

Twenty-four healthy male subjects (age: 26.79 ± 0.66 years) were included in the study. Subjects reported no psychiatric or neurological disorder. Written informed consent was obtained from all participants after the procedure had been fully explained. The study was approved by the Ethics Committee of the Charité–Universitätsmedizin Berlin.

### *Task*

*Individual pain stimulus selection.* Before the scanning session, subjects received 30 mild shocks of varying levels in randomized order and gave ratings on a visual analog scale (VAS) (Price et al., 1994; Brooks et al., 2010). The very left extreme of the VAS was labeled as 0 (not unpleasant at all); the very right extreme was labeled as 100 (worst imaginable unpleasantness) (Fig. 1*A*). For the tactile-stimulus application, we used a DS5 (Digitimer) stimulator controlled by a stimulation computer. A ring electrode was placed on the back of the left hand between thumb and index finger. For each subject, we fitted a power function to these ratings (Price et al., 1983) and defined five different pain stimuli with equal intervals in subjectively perceived unpleasantness (Fig. 1*B*). All visual and tactile stimuli as well as response recordings were controlled using Cogent2000 and MATLAB.

*Associating tactile stimuli with visual stimuli.* The set of five different pain stimuli obtained for each individual was then associated with five visual cues via a classical conditioning procedure. In each trial, a visual cue predicting a specific stimulus strength was presented for 1 s. After a 1 s delay, the corresponding tactile stimulus was applied to the subject in paired trials (80%), and no stimulation occurred in unpaired trials (20%). Each association was repeated 10 times (Fig. 1*C*).

*fMRI decision-making task.* fMRI acquisition consisted of four runs with 60 trials each. In each trial, subjects viewed one offer. The offer was a combination of a monetary amount and a visual pain cue that was learned previously. After a variable delay, subjects either accepted or rejected the offer by a left- or right-hand button press (Fig. 1*D*). Subjects were told that after the entire experiment, 15 trials of each run would be randomly selected and the accepted offers would be delivered to the subject (both money and pain), whereas the rejected offers would not. We had 12 monetary offers for each subject ranging from 1 to 99 cents (€) (mean 38 cent ± 2 SEM). For each subject, all combinations of money–pain cue pairs occurred equally often. All pain levels were paired with the complete range of monetary amounts. Before entering the scanner, subjects performed a practice version of the task from which the range of monetary offers was selected for each subject, ensuring that a similar number of offers would be accepted as well as rejected.

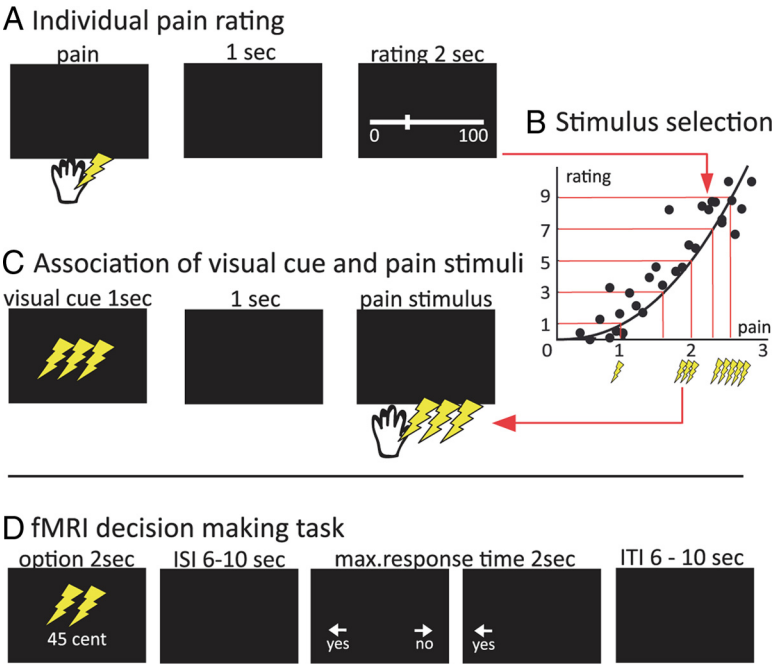


**Figure 1.** Multiattribute decision-making task. ***A***, Subjects rated tactile stimulations of different strengths on a VAS. ***B***, To select five pain stimuli for each individual, we estimated individual power functions using the subjective unpleasantness ratings. ***C***, The five selected pain stimuli were then associated with five different visual cues using a classical conditioning procedure. ***D***, fMRI experiment. In each trial, subjects saw an offer, which was a combination of a visual pain cue and an amount of money. After a variable delay, subjects either accepted or rejected the offer. Subjects were told that 15 trials would be randomly selected at the end of the experiment and both money and pain would be given in case the selected trial was an accepted offer and that they would receive nothing if it was a rejected offer. ISI, Interstimulus interval; ITI, intertrial interval.

### *Subjective value models and behavioral analysis*

The subjective value models integrated pain and money either independently or they additionally assumed an interaction between both attributes. The interactive term can be thought of as modulating the slope of the value of money as a function of pain. It quantifies by how much the increase in money (i.e., 1 to 99 cents) paired with low pain differs from the same monetary increase paired with high pain (Fig. 2*A–D*). Behavioral studies have suggested nonlinear value functions that allow concavity for positive values and convexity for negative values (Kahneman and Tversky, 1979). For completeness, we modeled the value functions for pain and money in both a linear and nonlinear manner. We refer to these models as (1) linear independent, (2) nonlinear independent, (3) linear interactive, and (4) nonlinear interactive (Fig. 2*A–D*). Mathematically, all models can be represented as a special case of the nonlinear interactive model, which defines the subjective value of a choice option $x$ by the subjective value of the monetary amount and the pain level of the option:

$$SV(x) = \beta_m m_x^{\alpha_m} + \beta_p p_x^{\alpha_p} + \beta_{mp} m_x^{\alpha_m} p_x^{\alpha_p},$$

where SV is the subjective value, $m_x$ is the monetary amount, $p_x$ is the pain level, and the $\beta$s represent the weights for money, pain, and the interaction, from left to right. The shape of the value functions for pain and money is modulated by an exponent $\alpha$ and thus allowed to deviate from linearity ($\alpha = 1$) to be concave ($\alpha < 1$) or convex ($\alpha > 1$). In case the weight $\beta_{mp}$ for the interaction of pain and money is set to zero, Equation 1 represents the two independent models (Fig. 2*A*,*B*), and in case the exponent for the value functions is 1, Equation 1 represents the two linear models (Fig. 2*A*,*C*). For all models, we assumed that the probability of accepting an option is a monotonic function of the options' subjective value, as defined by the soft-max choice rule:

$$p(accept\ x) = \frac{1}{1 + e^{-\pi \cdot SV(x)}},$$

where $\pi$ is a sensitivity parameter defining the slope of the sigmoid function, that is, the choices' stochasticity (the percentage of accepted offers plotted as a function of subjective value of the nonlinear independent model for demonstration; Fig. 2*F*).

Individual model parameters were estimated using a leave-one-out cross-validation procedure by minimizing the mean squared errors (MSE: average squared difference between the model prediction and subjects' actual choice behavior). Data from three runs were used to fit the free

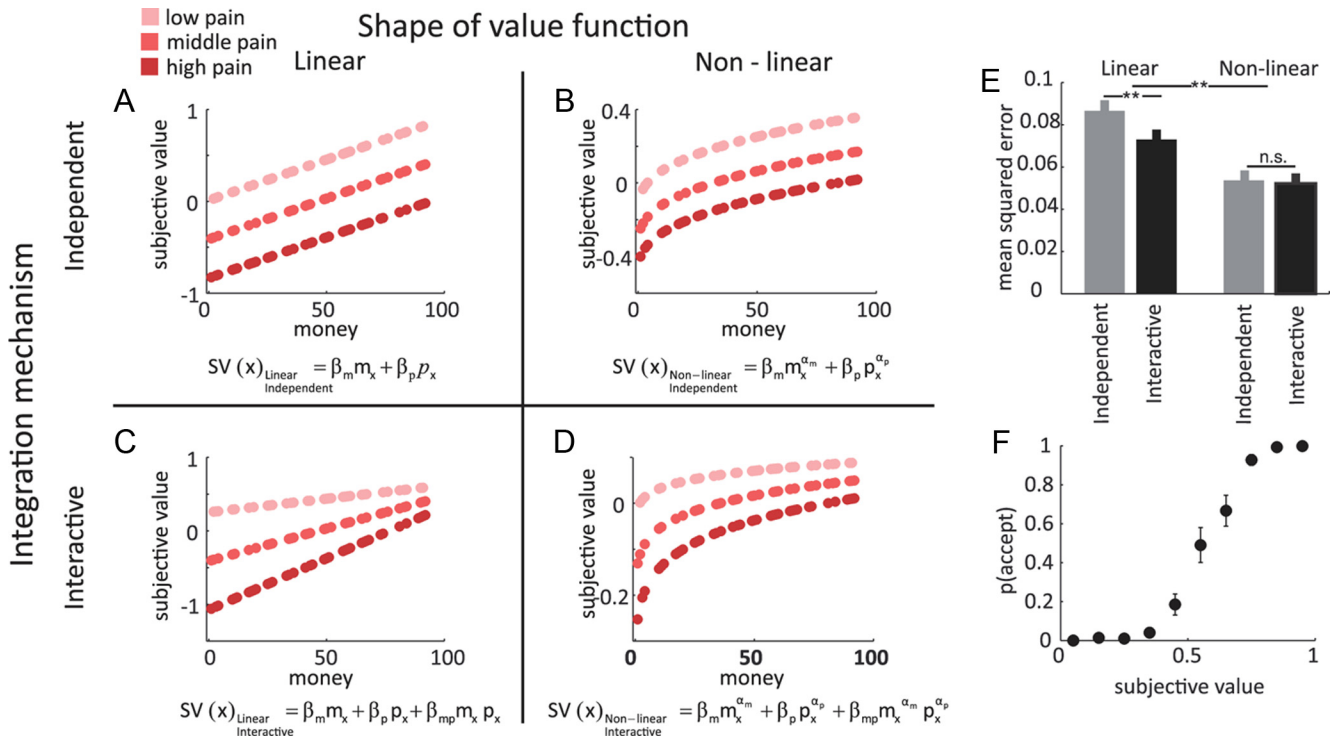


**Figure 2.** Subjective values of the four models. The subjective values (SV) of the corresponding model as a function of money are plotted. Color of the data points indicates the level of pain (i.e., the darker the points, the higher the pain level). ***A***, Linear independent; ***B***, nonlinear independent; ***C***, linear interactive; ***D***, nonlinear interactive. In the interactive models (***C***, ***D***), the subjective values from different pain levels are not only shifted on the *y*-axis but also have different slopes, that is, the difference between high money versus low money is modulated depending on the combined pain level (data from one subject for demonstration). ***E***, MSE of the four models in predicting choice behavior. When value functions were modeled in a linear fashion, the interactive models predicted the choice behavior better compared with the independent models ($t_{(23)} = 4.17$, $p < 0.0001$). However, when value functions were modeled nonlinearly, both integration mechanisms did not differ substantially ($t_{(23)} = 1.28$, $p = 0.21$). Note that the better predicting model has smaller MSE. Error bars indicate SEM. ***F***, The probability to accept increases as a function of subjective value (nonlinear interactive model). Error bars indicate SEM.

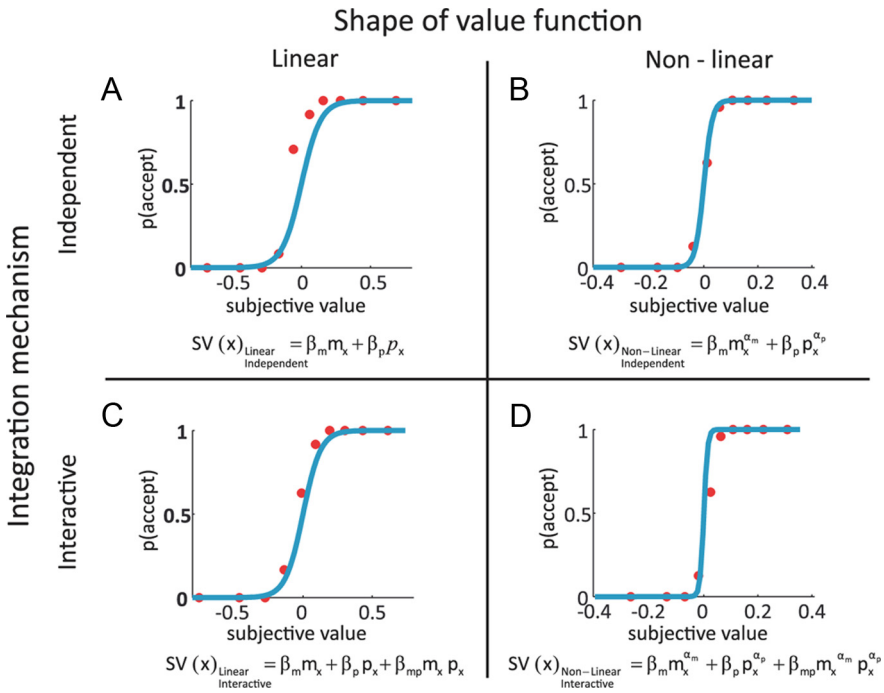


**Figure 3.** Predicted and actual percentage of accepted offers. The probability to accept plotted as a function of the subjective values (SV) derived from the four models. Blue lines indicate the model predictions and red dots indicate the actual choice behavior (percentages of accepted offers, binned in 10 categories). Data of a single subject are shown for illustration. ***A***, Linear independent; ***B***, nonlinear independent; ***C***, linear interactive; ***D***, nonlinear interactive.

model parameters, and their prediction accuracy was computed on the fourth independent test run. This procedure was repeated four times, each time using a different run as the independent test dataset. The prediction accuracy of a given model was defined as the average MSE in predicting the independent test data across all four cross-validation steps. This procedure allowed us to compare the MSE of four models against each other in predicting choice behavior, independent of the models' complexities (i.e., number of free parameters) (Stone, 1974; Hampton et al., 2008). MSE scores did not significantly deviate from a normal distribution (Kolmogorov–Smirnov test, all *p* values $> 0.7$). We thus compared the models' ability to predict choice behavior using a $2 \times 2$ ANOVA (integration mechanism $\times$ shape of value function).

### *fMRI acquisition and preprocessing*

Functional imaging was conducted on a 3 tesla Siemens Trio scanner with 12-channel head coil. In each of the four runs, 465 T2*-weighted gradient-echo EPIs containing 33 slices (3 mm thick) separated by a gap of 0.75 mm were acquired. Imaging parameters were as follows: TR = 2000 ms, TE = 30 ms, flip angle = 90°, matrix size = $64 \times 64$, and FOV = 192 mm, voxel size = $3 \times 3 \times 3.75$ mm.

Functional data were analyzed using SPM5 (Wellcome Department of Imaging Neuroscience). The first three volumes of each run were

discarded to allow for magnetic saturation effects. Images were slice time corrected, realigned, spatially normalized to a standard T2* template of MNI, resampled to 3 mm isotropic voxels, and spatially smoothed using an 8 mm FWHM Gaussian kernel. All included subjects moved less than the size of a single voxel (3 mm; maximal between-scan movement in mm, mean ± SEM, $x = 0.15 \pm 0.02$; $y = 0.36 \pm 0.04$; $z = 0.61 \pm 0.1$; in radians, mean ± SEM, pitch = 0.0087 ± 0.0025; roll = 0.0031 ± 0.0004; yaw = 0.0025 ± 0.0003).

### *Model-based fMRI data analysis*

To test the four models against each other at the neural level, for each subject, we set up a GLM with a parametric design (Büchel et al., 1998) for each subjective value model, resulting in four GLMs per subject. Each GLM had three regressors of interest: (1) onset of the offer, (2) the trial-wise subjective value of the offer, and (3) response onset. The subjective value regressor was created by parametrically modulating the stimulus function of the offer onset by the standardized (mean = 0, SD = 1) trial-wise subjective values derived from the four models. The regressors were convolved with a canonical HRF and orthogonalized with respect to the offer onset. All regressors were simultaneously regressed against the BOLD signal in each voxel. The regressors for offer and response onset are identical in all subjective value models; thus, the individual *t* maps of the subjective value regressors are proportional to the amount of variance in the BOLD response that is explained solely by each of the subjective value models in each voxel (i.e., effect size). The *t* maps of all four models were taken to a second-level random effect analysis.

First, to identify brain regions significantly correlating with the average of all four subjective value models, the four effect size images were averaged and tested ($p < 0.001$, uncorrected, $k = 10$). Second, analogous to the behavioral comparison, we set up a second-level random effect analysis, using a 2 × 2 ANOVA. Because the aim of this study was to identify which integration mechanism is used by the brain, the important comparison is the difference between interactive and independent models (and vice versa, collapsing across the value function shapes). The same procedure was applied to compare nonlinear and linear subjective values on the neural level. For this analysis, we applied a threshold of $p < 0.005$, $k = 5$, uncorrected within the mask of the average map of subjective values ($p < 0.05$). After having identified the regions in which changes in BOLD signal were significantly better predicted by the interactive models compared with independent models, we extracted the effect sizes of this region. We then performed *post hoc t* tests to investigate whether the interactive models made better predictions also for both linear and nonlinear value functions separately.

Finally, to resolve the question that could not be answered with the behavioral data, namely the superiority of the integration mechanism within the nonlinear models, we compared the effect sizes of the nonlinear interactive and the nonlinear independent models on a whole brain level using voxelwise paired *t* tests ($p < 0.001$, uncorrected).

### *Task-dependent changes in connectivity with the sgACC*

We performed a whole-brain psychophysiological interaction (PPI) analysis (Friston et al., 1997; Kahnt et al., 2009; Park et al., 2010) with the sgACC as a seed region. After having shown that the sgACC is involved in interactive value integration, we aimed to investigate how the interaction between pain and money actually modulates the effective connectivity of the sgACC with any other brain region. In contrast to the standard PPI analysis with only one psychological factor, we set up a PPI using two psychological factors (pain and money). We then searched for changes in effective connectivity with the interaction of pain and money. We first sorted all trials according to their pain and money levels into nine classes (3 money [low, middle, and high] × 3 pain [low (levels 1 and 2), middle (level 3), and high (levels 4 and 5)]). We extracted the entire time series from each subject in the cluster of the sgACC, in which activity showed significantly higher correlation with subjective values of the interactive models compared with that of the independent models (see Results, Neural representation of different subjective values). We first created regressors for each of the three pain levels. Within each of these three regressors, we coded the three money levels; that is, six TRs following the onset of high money trials were coded as 1, whereas six TRs following the

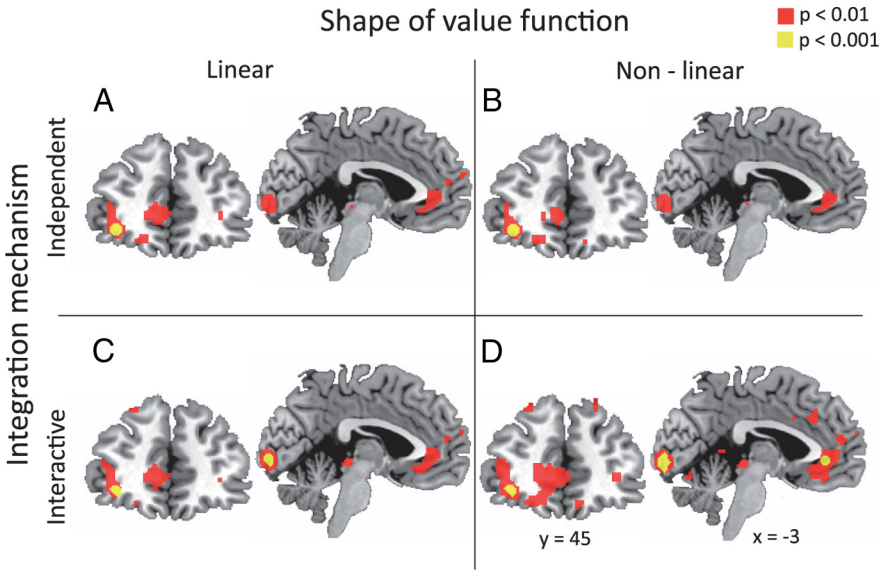


**Figure 4.** Brain regions encoding the subjective value of the four models. ***A***, Linear independent; ***B***, nonlinear independent; ***C***, linear interactive; ***D***, nonlinear interactive. Slices represent coronal (left) and sagittal (right) views of structural brain images with superimposed statistical maps.

**Table 1. Average effects of subjective values ($p < 0.001$, $k = 10$)**

| Region name | | BA | MNI *x* | MNI *y* | MNI *z* | *t* value |
|---|---|---|---|---|---|---|
| L | OFC | 11 | −21 | 33 | −15 | 3.83 |
| | Medial OFC | 32 | 0 | 39 | −3 | 3.69 |
| L | Central OFC | 10 | −36 | 48 | −6 | 4.39 |
| R | dlPFC | 8 | 42 | 30 | 51 | 4.09 |
| L | dlPFC | 8 | −24 | 36 | 54 | 3.67 |
| L | Parietal cortex | 7 | −24 | −63 | 54 | 3.67 |
| R | Parietal cortex | 40 | −51 | −42 | 57 | 3.43 |
| L | Occipital lobe | 18 | −12 | −96 | 6 | 7.70 |
| R | Occipital lobe | 18 | 27 | −99 | −6 | 4.39 |
| L | Cerebellum | | −27 | −81 | −48 | 3.65 |
| R | Cerebellum | | 42 | −81 | −33 | 4.18 |

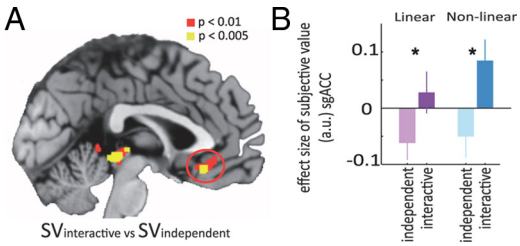


**Figure 5.** sgACC is involved when value affects valuation. ***A***, sgACC (0, 27, −15) showing significantly larger effect sizes for the subjective values (SV) of the interactive compared with the independent models in a direct whole-brain model comparison. Slice represents the sagittal view of structural brain image with superimposed statistical map. ***B***, This difference was also significant when testing the linear and nonlinear models separately. Error bars indicate SEM.

**Table 2. Comparison between interactive and independent models [collapsed across the curvature of value function; $p < 0.005$, $k = 5$, masked with the average map of subjective values ($p < 0.05$)]**

| Region name | | BA | MNI x | MNI y | MNI z | *t* value |
|---|---|---|---|---|---|---|
| | sgACC | 25 | 0 | 27 | −15 | 2.87 |
| R | dlPFC | 8 | 42 | 33 | 42 | 3.43 |
| R | OFC | 11 | 12 | 39 | −21 | 3.23 |
| L | Inferior parietal cortex | 40 | −42 | −42 | 48 | 2.82 |
| R | Inferior parietal cortex | 40 | 45 | −42 | 57 | 2.82 |
| L | Cerebellum | 11 | −36 | −48 | −30 | 3.16 |
| R | Thalamus | | 6 | −15 | 9 | 3.12 |
| | Periaqueductal grey | | 3 | −33 | −6 | 3.45 |
| R | Precentral cortex | 6 | 54 | −6 | 54 | 2.89 |
| L | Angular gyrus | 7 | 36 | −63 | 48 | 2.80 |
| L | Middle occipital gyrus | 37 | −51 | −63 | 20 | 3.31 |
| L | Occipital lobe | 19 | −27 | −66 | 42 | 3.10 |
| R | Occipital lobe | 19 | 36 | −81 | 21 | 2.89 |

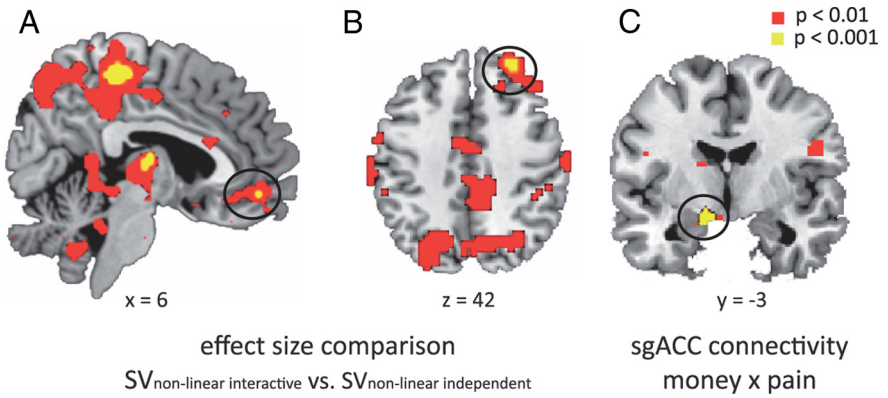


**Figure 6.** Whole-brain direct comparison between nonlinear interactive versus nonlinear independent models (***A***, ***B***) and the whole-brain effective connectivity of sgACC (***C***). ***A***, ***B***, Brain regions showing significantly larger effect sizes for the nonlinear interactive model compared with the nonlinear independent model. Slices represent sagittal (left) and transversal (right) views of structural brain images with superimposed statistical maps. The circled areas indicate anterior vmPFC [BA 11 (6, 48, −9), $t_{(92)} = 3.18$, $p < 0.001$] (***A***) and dlPFC [BA 9 (30, 45, 42), $t_{(92)} = 3.78$, $p < 0.001$] (***B***). ***C***, Functional connectivity between sgACC and left amygdala is enhanced as a function of money offers within the high-pain compared with the low-pain condition [(−12, −3, −12), $t_{(69)} = 4.14$, $p < 0.001$; coronal view of structural brain image with superimposed statistical map].

**Table 3. Nonlinear interactive > nonlinear independent ($p < 0.001$, $k = 10$)**

| Region name | | BA | MNI x | MNI y | MNI z | *t* value |
|---|---|---|---|---|---|---|
| R | OFC | 10/11 | 6 | 48 | −9 | 3.18 |
| R | dlPFC | 8 | 30 | 45 | 42 | 3.78 |
| R | Posterior cingulate cortex | 6 | 3 | −30 | 57 | 3.81 |
| L | Posterior cingulate cortex | 6 | −3 | −30 | 72 | 3.42 |
| R | Occipital lobe | 19 | −33 | −78 | 27 | 3.77 |
| R | Thalamus | | 12 | −12 | 9 | 3.57 |
| L | Cerebellum | | −36 | −48 | −30 | 3.48 |
| L | Midbrain | | −12 | −12 | −27 | 3.37 |
| L | Parietal cortex | 7 | −27 | −78 | 45 | 3.33 |
| R | Temporal cortex | 37 | 51 | −63 | −18 | 3.32 |
| R | Midfrontal cortex | 6 | 36 | 6 | 60 | 3.30 |
| L | Precentral gyrus | 6 | −30 | −9 | 60 | 3.47 |
| L | Parahippocampal gyrus | 30 | −21 | −36 | −15 | 3.25 |
| R | Parahippocampal gyrus | 30 | 21 | −24 | −18 | 3.23 |

onset of low money trials were coded as −1, and the middle money trials were coded with zeros. The time window of six TRs was selected to capture the entire hemodynamic response function (Kahnt et al., 2009; Park et al., 2010). These regressors were then multiplied by the normalized time series of sgACC. Thus, for each pain level, the resulting regressor represents the interaction between sgACC activity and money for one pain level. The middle regressors of pain and money were included in the single-subject model, but were not used to compute the group contrasts because of the smaller number of trials in these classes. Importantly, the created PPI regressors were used as covariates in a separate regression, which also included all the psychological regressors [three onset regressors for three pain levels, each regressor coding the onset of high money (as +1), middle money (as 0), and low money (as −1), convolved with an HRF] and the physiological regressor (the entire time series of sgACC). Because the seed region is defined (the contrast interactive vs independent) in a similar way as the psychological factor of the PPI regressors (interaction between pain and money), the psychological, PPI, and physiological regressors may be correlated. Note that this deviates from the standard PPI approach, in which the seed ROI definition is usually orthogonal to the psychological factor. However, because we entered all regressors simultaneously into the model, the shared variance would not be attributed to any of the regressors. According to this, the PPI regressor explains the incremental variance that is neither explained by the psychological regressors nor by the physiological regressor. Individual contrast images for sgACC connectivity modulated by money for high-pain and low-pain levels were then entered into second-level *t* tests.

## Results

### Model predictions on choice behavior

The Kolmogorov–Smirnov test revealed that all MSEs did not differ from normal distributions (*p* values for MSE linear independent = 0.996; linear interactive = 0.877; nonlinear independent = 0.993; nonlinear interactive = 0.734). A 2 × 2 ANOVA (integration mechanism × shape of value function) with the four models revealed that the nonlinear models had higher predictive power compared with the linear models ($F_{(1,23)} = 17.17$, $p < 0.001$). However, we found a significant interaction effect ($F_{(1,23)} = 21.35$, $p < 0.001$) demonstrating the superiority of the interactive model over the independent model only when the value functions were modeled linearly. Within the nonlinear value functions, the predictive power of both integration mechanisms did not differ substantially ($t_{(23)} = 1.28$, $p = 0.21$) (Fig. 2*E*; Fig. 3*A–D* shows choice behavior of a single subject as a function of the subjective values derived from the four models). Thus, we conclude that, on the basis of choice behavior, it is not possible to identify the integration mechanism. Therefore, we further compared the predictive power of the models directly on neural data to gain insight into the underlying cognitive integration mechanism.

### Model-based fMRI data analysis

*Neural representation of different subjective values*

The four models showed similar patterns of correlation with BOLD responses (Fig. 4). On average, the subjective values of the four models showed significant correlation in the medial prefrontal cortex [mPFC (0, 39, −3), $t_{(92)} = 3.69$, $p < 0.001$], the central orbitofrontal cortex [cOFC (−36, 48, −6), $t_{(92)} = 4.39$, $p < 0.001$], and the dorsolateral prefrontal cortex [dlPFC (−24, 36, 54), $t_{(92)} = 3.67$, $p < 0.001$] (see Table 1 for whole-brain results).

Next, we performed a whole-brain model comparison by statistically testing the effect sizes of the different models. The interactive models showed significantly larger effect sizes in sgACC [BA 25 (0, 27, −15), $t_{(92)} = 2.87$, $p < 0.005$] compared with the independent models (collapsed across linear and nonlinear models) (Fig. 5*A*, see Table 2 for whole-brain results). In contrast, there were no voxels in which BOLD responses were better predicted by the subjective values of the independent models. Furthermore, we did not find any voxels in which BOLD responses were significantly better predicted by the subjective values of the nonlinear compared with the linear models or vice versa.

A *post hoc* ROI analysis revealed that in the sgACC, the effect sizes of the interactive models were larger than those of the independent models in both linear and nonlinear models separately ($t_{(23)} = 2.47$, $p < 0.05$; $t_{(23)} = 2.87$, $p < 0.05$, respectively) (Fig. 5*B*). Thus, we conclude that values are integrated by means of an interactive integration mechanism and that sgACC plays a crucial role in this function.

*Identifying the neural integration mechanism*

We have shown that both nonlinear models made better behavioral predictions than the two linear models. However, within the nonlinear models, both integration mechanisms (interactive and independent) predicted choice behavior equally well (see above). Therefore, we used the brain data to identify which of the nonlinear integration mechanisms is superior in predicting the BOLD signal in value-sensitive brain regions. Thus, this analysis can serve as a tiebreaker between competing models of brain processes underlying decision making. The nonlinear interactive model revealed voxels with higher effect sizes than the nonlinear independent model in the medial OFC [(6, 48, −9), $t_{(92)} = 3.18$, $p < 0.001$] and the dlPFC [(30, 45, 42), $t_{(92)} = 3.78$, $p < 0.001$] as well as other regions (Fig. 6*A*,*B*, Table 3). In contrast, we did not find any voxel in which BOLD changes were significantly better predicted by the nonlinear independent model compared with the nonlinear interactive model. Hence, we conclude that the nonlinear interactive model provides the better description of the neural processes underlying choice behavior among multiattribute options.

**Effective connectivity of sgACC**

Finally, the whole-brain PPI analysis with the sgACC as seed region revealed a significant difference in the money-dependent connectivity modulation when contrasting high versus low pain in the amygdala/sublenticular extended amygdala (SLEA) [(−12, −3, −12), $t_{(69)} = 4.14$, $p < 0.001$] (Fig. 6*C*).

## Discussion

In the present study, we showed that value affects valuation when advantages and disadvantages are integrated into an overall subjective value. This study provides a concrete example of how neuroimaging directly allows one to test between computational models of decision making and facilitates the evaluation of cognitive computations. Thus, our study supports the promise of neuroeconomics that neuroimaging can significantly contribute to the evaluation of economic questions.

Although independent and interactive subjective value models rely on different assumptions, both models make very similar predictions about the choice behavior. Indeed, in our case, the interactive and independent models performed equally well in predicting subjects' behavior when the value functions were modeled nonlinearly. Thus, behavioral data alone were insufficient to conclude which integration mechanism (interactive vs independent) best describes the cognitive process of integrating the attributes' values into the subjective value of multiattribute options. Therefore, we went on to compare the predictive power of the models on the neural data. This revealed that interactive models are superior to the independent models in predicting neural activity in the sgACC, independent of the curvature of the value functions. Thus, this analysis of neural activation provides a potential solution for the computational mechanisms of value integration, for which behavioral measures in this study were not informative. Only a few studies so far have compared different models directly on neural data (Hampton et al., 2006, 2008; Montague et al., 2006; Kable and Glimcher, 2007; Rangel et al., 2008). This approach is related to some model-based fMRI studies (Breiter et al., 2001; O'Doherty et al., 2004; Seymour et al., 2004; Kim et al., 2006; Talmi et al., 2009) and provides a concrete example of using neural signals with modeling to identify integration computations that cannot be easily identified by behavioral measures. The identification of the better describing model is essential, even if the two models may yield similar patterns of prediction for choice behavior on one dataset, because this does not imply that this will be the case in other decision situations. Specifically, it is important to identify more accurate descriptions of the underlying process because such models will make new and more precise predictions in future and alternative situations (see also Camerer, 2007). In line with this, future studies should create decision situations in which those models make diverging predictions and compare the models' accuracy in predictions.

Finally, we showed that the connectivity between the sgACC and the amygdala/SLEA was modulated as a function of money only during high-pain conditions. This suggests that interactive value integration relies on the interplay between the sgACC and the amygdala/SLEA.

Subjective values of all four models showed significant correlations with the BOLD signal in medial PFC and OFC. This is in line with evidence suggesting that the ventral part of the medial PFC and OFC encodes the reward value of choice options (Aharon et al., 2001; Daw et al., 2006; Kim et al., 2006; Plassmann et al., 2008; Gasic et al., 2009; Hare et al., 2009; Kahnt et al., 2010, 2011; Philiastides et al., 2010; Smith et al., 2010). Talmi and colleagues (2009) have demonstrated that activity in this region increases with rewards and is attenuated by the prospect of pain. Furthermore, our result that sgACC, together with the amygdala/SLEA, is involved in interactively modulating hedonic experience is consistent with a large body of evidence from cognitive neuroscience. In studies investigating monetary gains and losses, Breiter et al. (2001) have reported that SLEA activity is modulated not only by the prospect of monetary gains and losses but also by their outcomes. In monkeys and rats, analogous regions are involved in regulating fear by exerting inhibitory control over amygdala activity (Sotres-Bayon et al., 2004; Quirk and Beer, 2006; Milad and Rauch, 2007). Studies on fear extinction in rats have shown that stimulating this PFC region modulates amygdala responses, thereby affecting the expression of conditioned responding (Quirk et al., 2003; Rosenkranz et al., 2003). In humans, during extinction and the regulation of learned negative values, the sgACC is actively engaged together with the amygdala independent of the modulation strategy (Phelps et al., 2004; Etkin et al., 2006; Delgado et al., 2008; Schiller and Delgado, 2010). Similarly, sgACC–amygdala coupling is involved in pain regulation such as placebo analgesia and pain habituation (Mayberg et al., 2002; Bingel et al., 2006, 2007). An interesting question is whether our results can be generalized to other types of cost–benefit integra-

tion. Recent evidence suggests distinct valuation subsystems for different types of costs and benefits. For example, Prévost et al. (2010) have shown that delay and effort discounting engage different neural circuits (see also Croxson et al., 2009). Also, besides sgACC and amygdala, ventromedial PFC, and striatum have been shown to play a key role in initial acquisition and modulation of the fear response (Schiller and Delgado, 2010).

In summary, the present study compared different subjective value models with independent and interactive value integration mechanisms directly on fMRI data. This procedure provided neural evidence that an interactive rather than an independent integration mechanism is implemented in the brain. Furthermore, it suggests that the sgACC, in concert with the amygdala, is critically involved in this process. By demonstrating how different values are integrated in the brain, our results substantially extend our knowledge about the neurobiological underpinnings of human choice behavior. Moreover, they contribute to the field of neuroeconomics by showing that direct model comparisons on brain data can be used to uncover cognitive processes and thereby to decide among competing models of decision making.

## References


Aharon I, Etcoff N, Ariely D, Chabris CF, O'Connor E, Breiter HC (2001) Beautiful faces have variable reward value: fMRI and behavioral evidence. Neuron 32:537–551.

Becerra L, Breiter HC, Wise R, Gonzalez RG, Borsook D (2001) Reward circuitry activation by noxious thermal stimuli. Neuron 32:927–946.

Bhatt MA, Lohrenz T, Camerer CF, Montague PR (2010) Neural signatures of strategic types in a two-person bargaining game. Proc Natl Acad Sci U S A 107:19720–19725.

Bingel U, Lorenz J, Schoell E, Weiller C, Büchel C (2006) Mechanisms of placebo analgesia: rACC recruitment of a subcortical antinociceptive network. Pain 120:8–15.

Bingel U, Schoell E, Herken W, Büchel C, May A (2007) Habituation to painful stimulation involves the antinociceptive system. Pain 131:21–30.

Blood AJ, Zatorre RJ, Bermudez P, Evans AC (1999) Emotional responses to pleasant and unpleasant music correlate with activity in paralimbic brain regions. Nat Neurosci 2:382–387.

Breiter HC, Etcoff NL, Whalen PJ, Kennedy WA, Rauch SL, Buckner RL, Strauss MM, Hyman SE, Rosen BR (1996) Response and habituation of the human amygdala during visual processing of facial expression. Neuron 17:875–887.

Breiter HC, Aharon I, Kahneman D, Dale A, Shizgal P (2001) Functional imaging of neural responses to expectancy and experience of monetary gains and losses. Neuron 30:619–639.

Brooks AM, Pammi VS, Noussair C, Capra CM, Engelmann JB, Berns GS (2010) From bad to worse: striatal coding of the relative value of painful decisions. Front Neurosci 4:176.

Bruni L, Sugden R (2007) The road not taken: how psychology was removed from economics, and how it might be brought back. Econ J 117:146–173.

Büchel C, Holmes AP, Rees G, Friston KJ (1998) Characterizing stimulus-response functions using nonlinear regressors in parametric fMRI experiments. Neuroimage 8:140–148.

Camerer CF (2007) Neuroeconomics: using neuroscience to make economic predictions. Econ J 117:C26–C42.

Croxson PL, Walton ME, O'Reilly JX, Behrens TE, Rushworth MF (2009) Effort-based cost–benefit valuation and the human brain. J Neurosci 29:4531–4541.

Daw ND, O'Doherty JP, Dayan P, Seymour B, Dolan RJ (2006) Cortical substrates for exploratory decisions in humans. Nature 441:876–879.

Delgado MR, Nearing KI, Ledoux JE, Phelps EA (2008) Neural circuitry underlying the regulation of conditioned fear and its relation to extinction. Neuron 59:829–838.

Etkin A, Egner T, Peraza DM, Kandel ER, Hirsch J (2006) Resolving emotional conflict: a role for the rostral anterior cingulate cortex in modulating activity in the amygdala. Neuron 51:871–882.

Friston KJ, Buechel C, Fink GR, Morris J, Rolls E, Dolan RJ (1997) Psychophysiological and modulatory interactions in neuroimaging. Neuroimage 6:218–229.

Gasic GP, Smoller JW, Perlis RH, Sun M, Lee S, Kim BW, Lee MJ, Holt DJ, Blood AJ, Makris N, Kennedy DK, Hoge RD, Calhoun J, Fava M, Gusella JF, Breiter HC (2009) BDNF, relative preference, and reward circuitry responses to emotional communication. Am J Med Genet B Neuropsychiatr Genet 150B:762–781.

Glimcher PW, Rustichini A (2004) Neuroeconomics: the consilience of brain and decision. Science 306:447–452.

Hampton AN, Bossaerts P, O'Doherty JP (2006) The role of the ventromedial prefrontal cortex in abstract state-based inference during decision making in humans. J Neurosci 26:8360–8367.

Hampton AN, Bossaerts P, O'Doherty JP (2008) Neural correlates of mentalizing-related computations during strategic interactions in humans. Proc Natl Acad Sci U S A 105:6741–6746.

Hare TA, Camerer CF, Rangel A (2009) Self-control in decision-making involves modulation of the vmPFC valuation system. Science 324:646–648.

Huber GP (1974) Multi-attribute utility models—review of field and field-like studies. Manage Sci 20:1393–1402.

Kable JW, Glimcher PW (2007) The neural correlates of subjective value during intertemporal choice. Nat Neurosci 10:1625–1633.

Kahneman D, Tversky A (1979) Prospect theory—analysis of decision under risk. Econometrica 47:263–291.

Kahnt T, Park SQ, Cohen MX, Beck A, Heinz A, Wrase J (2009) Dorsal striatal-midbrain connectivity in humans predicts how reinforcements are used to guide decisions. J Cogn Neurosci 21:1332–1345.

Kahnt T, Heinzle J, Park SQ, Haynes JD (2010) The neural code of reward anticipation in human orbitofrontal cortex. Proc Natl Acad Sci U S A 107:6010–6015.

Kahnt T, Heinzle J, Park SQ, Haynes JD (2011) Decoding different roles for vmPFC and dlPFC in multi-attribute decision making. Neuroimage. 56:709–715.

Keeney R, Raiffa H (1976) Decisions with multiple objectives: preferences and value tradeoffs. New York: Wiley.

Kim H, Shimojo S, O'Doherty JP (2006) Is avoiding an aversive outcome rewarding? Neural substrates of avoidance learning in the human brain. PLoS Biol 4:e233.

Loewenstein G, Rick S, Cohen JD (2008) Neuroeconomics. Annu Rev Psychol 59:647–672.

Mayberg HS, Silva JA, Brannan SK, Tekell JL, Mahurin RK, McGinnis S, Jerabek PA (2002) The functional neuroanatomy of the placebo effect. Am J Psychiatry 159:728–737.

Mazur JE, Biondi DR (2009) Delay-amount tradeoffs in choices by pigeons and rats: hyperbolic versus exponential discounting. J Exp Anal Behav 91:197–211.

Milad MR, Rauch SL (2007) The role of the orbitofrontal cortex in anxiety disorders. Ann N Y Acad Sci 1121:546–561.

Montague PR, King-Casas B, Cohen JD (2006) Imaging valuation models in human choice. Annu Rev Neurosci 29:417–448.

Navalpakkam V, Koch C, Rangel A, Perona P (2010) Optimal reward harvesting in complex perceptual environments. Proc Natl Acad Sci U S A 107:5232–5237.

O'Doherty J, Dayan P, Schultz J, Deichmann R, Friston K, Dolan RJ (2004) Dissociable roles of ventral and dorsal striatum in instrumental conditioning. Science 304:452–454.

O'Doherty JP, Hampton A, Kim H (2007) Model-based fMRI and its application to reward learning and decision making. Ann NY Acad Sci 1104:35–53.

Park SQ, Kahnt T, Beck A, Cohen MX, Dolan RJ, Wrase J, Heinz A (2010) Prefrontal cortex fails to learn from reward prediction errors in alcohol dependence. J Neurosci 30:7749–7753.

Phelps EA, Delgado MR, Nearing KI, LeDoux JE (2004) Extinction learning in humans: role of the amygdala and vmPFC. Neuron 43:897–905.

Philiastides MG, Biele G, Heekeren HR (2010) A mechanistic account of value computation in the human brain. Proc Natl Acad Sci U S A 107:9430–9435.

Plassmann H, O'Doherty J, Shiv B, Rangel A (2008) Marketing actions can modulate neural representations of experienced pleasantness. Proc Natl Acad Sci U S A 105:1050–1054.

Plassmann H, O'Doherty JP, Rangel A (2010) Appetitive and aversive goal values are encoded in the medial orbitofrontal cortex at the time of decision making. J Neurosci 30:10799–10808.

Prévost C, Pessiglione M, Météreau E, Cléry-Melin ML, Dreher JC (2010)

Separate valuation subsystems for delay and effort decision costs. J Neurosci 30:14080–14090.
Price DD, McGrath PA, Rafii A, Buckingham B (1983) The validation of visual analogue scales as ratio scale measures for chronic and experimental pain. Pain 17:45–56.
Price DD, Bush FM, Long S, Harkins SW (1994) A comparison of pain measurement characteristics of mechanical visual analogue and simple numerical rating scales. Pain 56:217–226.
Quirk GJ, Beer JS (2006) Prefrontal involvement in the regulation of emotion: convergence of rat and human studies. Curr Opin Neurobiol 16:723–727.
Quirk GJ, Likhtik E, Pelletier JG, Paré D (2003) Stimulation of medial prefrontal cortex decreases the responsiveness of central amygdala output neurons. J Neurosci 23:8800–8807.
Rangel A, Camerer C, Montague PR (2008) A framework for studying the neurobiology of value-based decision making. Nat Rev Neurosci 9:545–556.
Rosenkranz JA, Moore H, Grace AA (2003) The prefrontal cortex regulates lateral amygdala neuronal plasticity and responses to previously conditioned stimuli. J Neurosci 23:11054–11064.
Sanfey AG, Loewenstein G, McClure SM, Cohen JD (2006) Neuroeconomics: cross-currents in research on decision-making. Trends Cogn Sci 10:108–116.
Schiller D, Delgado MR (2010) Overlapping neural systems mediating extinction, reversal and regulation of fear. Trends Cogn Sci 14:268–276.
Seymour B, O'Doherty JP, Dayan P, Koltzenburg M, Jones AK, Dolan RJ, Friston KJ, Frackowiak RS (2004) Temporal difference models describe higher-order learning in humans. Nature 429:664–667.
Smith DV, Hayden BY, Truong TK, Song AW, Platt ML, Huettel SA (2010) Distinct value signals in anterior and posterior ventromedial prefrontal cortex. J Neurosci 30:2490–2495.
Sotres-Bayon F, Bush DE, LeDoux JE (2004) Emotional perseveration: an update on prefrontal-amygdala interactions in fear extinction. Learn Mem 11:525–535.
Stone M (1974) Cross-validatory choice and assessment of statistical predictions. J R Statist Soc Series B Stat Methodol 36:111–147.
Talmi D, Dayan P, Kiebel SJ, Frith CD, Dolan RJ (2009) How humans integrate the prospects of pain and reward during choice. J Neurosci 29:14617–14626.
Wallenius J, Dyer JS, Fishburn PC, Steuer RE, Zionts S, Deb K (2008) Multiple criteria decision making, multiattribute utility theory: recent accomplishments and what lies ahead. Manage Sci 54:1336–1349.
Wiech K, Ploner M, Tracey I (2008) Neurocognitive aspects of pain perception. Trends Cogn Sci 12:306–313.

**Project II**

Park, S.Q., Kahnt, T.,Talmi, D., Rieskamp, J., Dolan,R.J., Heekeren, H.R. (2012)

Adaptive coding of reward prediction errors is gated by striatal coupling

*Proceedings of the National Academy of Sciences (PNAS), in press*

doi: 10.1073/pnas.1119969109

# Adaptive coding of reward prediction errors is gated by striatal coupling

Soyoung Q Park[a, b, 1], Thorsten Kahnt[b, c], Deborah Talmi[d],
Jörg Rieskamp[e], Raymond J. Dolan[d], Hauke R. Heekeren[a, b]

[a] Department of Education and Psychology, Freie Universität Berlin, Habelschwerdter Allee 45, 14195 Berlin, Germany
[b] Berlin School of Mind and Brain, Humboldt Universität zu Berlin, Luisenstraße 56, 10117 Berlin, Germany
[c] Bernstein Center for Computational Neuroscience, Charité - Universitätsmedizin Berlin, Phillipstraße 13, 10115 Berlin, Germany
[d] Wellcome Trust Centre for Imaging Neuroscience, University College London, 12 Queen Square, WC1N London, United Kingdom
[e] University of Basel, Department of Psychology, Missionsstrasse 62a, 4055 Basel, Switzerland

**Classification:**
BIOLOGICAL SCIENCES: Neuroscience, SOCIAL SCIENCE: Psychological & Cognitive Sciences

**[1]Corresponding Author**
Soyoung Q Park
Psychology of Emotion/Affective Neuroscience
Department of Education and Psychology
Freie Universität Berlin
Habelschwerdter Allee 45, 14195 Berlin
Germany
Tel. +49 30 838 57168
Fax. +49 30 838 55778
E-Mail. Soyoung.q.park@gmail.com

**Muscript Information:** 3 figures, 14 text pages

**Keywords:** normalization, dopamine, adjustment, functional connectivity, context invariance

**Author Contributions:** S.Q.P., D.T., H.R.H., R.J.D. designed the study. S.Q.P., T.K. performed the research. S.Q.P., T.K. analyzed the data. S.Q.P., T.K., J.R., R.J.D. H.R.H., wrote the paper.

**This manuscript is accepted for publication in *Proceedings of the National Academy of Sciences (PNAS).***
(doi: 10.1073/pnas.1119969109**)**

## Abstract

To efficiently represent all the possible rewards in the world, dopaminergic midbrain neurons dynamically adapt their coding range to momentarily available rewards. Specifically, these neurons increase their activity for an outcome that is better than expected and decrease it for a worse than expected, independent of absolute reward magnitude. Although this adaptive coding is well documented, it remains unknown precisely how this rescaling is implemented. To investigate this, we used human functional magnet resonance imaging (fMRI) in combination with a reward prediction task that involved different reward magnitudes. We demonstrate that reward prediction errors in the human striatum are expressed according to an adaptive coding scheme. Strikingly, we show that adaptive coding, a de facto context invariance, is gated by changes in effective connectivity between the striatum and other reward sensitive regions, namely the midbrain and medial prefrontal cortex. Our results provide evidence of how striatal prediction errors are normalized by a magnitude-dependent alteration in inter-regional connectivity within the brain reward system.

## Introduction

From receiving a piece of chocolate to winning a lottery, the range of possible rewards in the world is immense, yet the coding range of reward-sensitive neurons is limited. An efficient way for the brain to solve this problem is by dynamically adjusting the activity range of neurons according to the momentarily available rewards. Such an adaptive coding mechanism maximizes the discriminability between different values in a given reward context, thus enabling efficient information processing.

Specifically, adaptive coding of reward prediction errors (PEs) has been suggested by a wide range of theories from economics and reinforcement learning. A PE quantifies the mismatch between the expected and actually received reward. For example, when our expectation is to win 50€, but we win 30€ instead, there is a prediction error of -20€. However, in case our initial expectation was to win 20€, the prediction error will be +10€. Prospect theory suggests that changes are coded according to an individual reference outcome, such as the status quo or individual expectations (1, 2). In reinforcement learning theory, on the other hand, the PE is considered to be essential for updating the reward values associated with the predicting cue, thus acting as a teaching signal (3, 4).

Adaptive coding of PE is essential for two reasons. First, the reward magnitude (lottery or chocolate) is already encoded during expectation. Hence, in terms of effective neural coding, it is not necessary to represent the reward magnitude redundantly when computing the prediction errors. Second, in the context of learning, computing this quantity depending on reward magnitude would prohibit learning from small rewards. That is, no matter in what situation we are, only the prediction error of extremely high rewards would be behaviorally relevant and prediction errors of small rewards would never impact behavior. Indeed, animal recording studies have shown that dopaminergic midbrain neurons encode reward prediction errors (5, 6) according to an adaptive coding scheme (7). Specifically, these neurons increase their activity for the larger of two potential reward outcomes and decrease their activity for the smaller outcome independent of the absolute reward magnitude (7). Human studies using functional magnetic resonance imaging (fMRI) highlight PE-related

activity in the ventral striatum (8-14), activity often presumed to reflect a dopaminergic input from the midbrain.

Adaptive coding is a normalization process that brings different magnitudes onto the same coding scale. Although adaptive coding in reward-sensitive neurons is well documented (7, 15-17) it is unknown how the brain normalizes different ranges of rewards to enable the adaptive coding. One possible mechanism for such normalization is via modulation of connectivity with other reward coding areas, including areas that might show sensitivity to actual reward magnitudes. The major dopaminergic innervations to the striatum originates in the ventral tegmental area (VTA) and the substantia nigra (SN) (18). Additionally, there is a strong input from regions encoding reward value, notably orbitofrontal and ventromedial prefrontal cortex (OFC/vmPFC) (19-24). On this basis we hypothesized that changes in striatal connectivity with these regions would underlie an adjustment in the coding range of striatal PEs. Specifically, when a high reward magnitude is encountered, a dynamic change in connectivity would render striatal PE coding comparable to that of a lower reward magnitude.

Here, we aimed to investigate the normalization process underlying adaptive coding by means of fMRI. First, we addressed the question of whether prediction errors are represented according to an adaptive coding scheme in the human striatum. Second, we investigated how the brain implements the reward rescaling for adaptive coding.

Subjects performed a simple reward prediction task that induces PEs. In each trial, subjects saw a cue indicating the possible reward; in trials with high reward magnitude, subjects saw 1€ combined with either high or low probability (66% or 33%). In trials with low reward magnitude, subjects saw 10 Cents with high or low probability (Fig. 1*A*). The reward cues appeared either on the right or left side of the screen and subjects were asked to indicate the position of the reward cue using a button press. After a variable delay, subjects saw either the corresponding coin indicating the outcome was obtained, or they saw the coin with a superimposed cross indicating the outcome was omitted (Fig. 1*A*). Importantly, in our task, the reward magnitudes were combined with different probabilities that allowed us to disentangle PE related activity from outcome related activity.

## Results

**Behavioral Results.** Subjects correctly indicated the location of the cue in 99.33 ± 0.02 % of the trials. A two-by-two ANOVA (reward magnitude × probability) on the reaction time (RT) data revealed a significant main effect of magnitude ($F_{1,27}$=13.75, $P$<0.001) and a significant main effect of probability ($F_{1,27}$=12.67, $P$<0.001). There was no significant magnitude-by-probability interaction ($F_{1,27}$=1.73, $P$=0.2). Subjects responded faster in the high compared to low reward magnitude (high=555 ms, low=568 ms) and in the high compared to low probability trials (high=557 ms, low=567 ms) indicating that both reward magnitude and probability affected reward expectations independently (Fig. 1*B*).

**Neuroimaging Results.** Our first analysis of imaging data focused on the question of adaptive coding of prediction errors. We applied a whole-brain general linear model (GLM) that included onset regressors for the reward cue, outcome and two parametric regressors at the

time of reward outcome. The first parametric regressor coded outcome delivery as one for received and minus one for omitted rewards. The second parametric regressor accounted for the PE related variance and was orthogonalized with respect to the first parametric regressor. Hence, this PE regressor accounts for variance in the BOLD (brain-oxygen-level-dependent) signal that is independent of outcome-related activity. Voxel-wise one-sample t-tests on the parameter estimates of the parametric PE regressor revealed a significant correlation between PE and activity in the ventral striatum (Fig. 2*A*; $P < 0.05$, FWE small volume corrected (SVC), [-6 18, -3]; $t = 4.19$).

After having identified the region in ventral striatum coding reward prediction errors, we determined if this striatal region adaptively codes PE responses. Specifically we tested whether the striatal PE responses were invariant for different reward magnitudes. In case where prediction errors are coded according to an adaptive coding scheme, representations of striatal PEs for high reward should not differ from those of low reward. We applied a GLM to the striatal data, but this time all the regressors were split for high and low reward trials. The onset regressors for cue, outcome and the two parametric regressors for outcome-related variance and two PE coding regressors were regressed against the BOLD signal in the striatum. Both prediction-error regressors were orthogonalized with respect to the parametric modulation of reward outcome. This comparison of PE-related responses in high vs. low reward magnitudes revealed no significant difference in the striatum (Fig. 2*B*; $t_{27}$=-0.98, $P$=0.34).

We further performed an additional analysis in which we directly tested whether the striatal changes in BOLD signal are significantly better predicted by an adaptive PE (PE modulated only by probability) than by a non-adaptive PE (PE modulated by both probability and magnitude, i.e., their product). If an adaptive PE predicts striatal activity better than a non-adaptive PE, this would support adaptive PE coding in the striatum. In a case where prediction errors are modulated by reward magnitude, then a non-adaptive PE would provide a better prediction of striatal activity. Importantly, our analysis shows that the striatal BOLD signal is significantly better predicted by an adaptive, compared to a non-adaptive PE (Fig. 2*C*; $t_{27}$=2.82, $P$=0.0089; mean parameter estimates for adaptive PE: 0.37±0.014; non-adaptive PE: 0.29±0.018). This invariance in the representation of striatal PEs is consistent with an adaptive coding scheme shown in dopaminergic neurons in primates (7).

Having shown that PEs are adaptively coded in the striatum, our next analysis sought to determine whether there were dynamic changes in striatal coupling associated with this magnitude-dependent rescaling. We hypothesized that reward sensitive brain regions with striatal innervations, specifically the vmPFC and the VTA/SN, would modulate striatal activity as a function of reward magnitude. To test this, we performed a whole-brain psychophysiological interaction analysis (PPI) where the entire striatal time series of PE-related activity (Fig. 3*A*) was selected as a physiological variable and the reward magnitude as a psychological variable (high vs. low reward). Comparing striatal connectivity between reward magnitudes revealed significant ($P$<0.001, k=10) modulations in the VTA/SN ([6 -8 -21]; $P < 0.05$, FWE SVC corrected, $t_{27}$=4.74, Fig. 3*B*) and the vmPFC ([3 54 -3], BA10/BA9; $P < 0.05$, FWE SVC corrected, $t_{27}$=4.85, Fig. 3*D*). Specifically, this reflected significant less coupling during the high compared to the low reward magnitude between the striatum and both VTA/SN and vmPFC, respectively (Fig. 3*C*).

## Discussion

From visual neurons (25, 26) to reward coding dopaminergic neurons, scale invariance is an ubiquitous encoding principle in the brain. Retinal neurons rapidly adapt to an enormous range of light to guarantee high visual discriminability. Dunn and colleagues (27) have shown that this adaptation is implemented via a relay from cone bipolar cells to ganglion cells. This demonstrates that such a rapid rescaling of range occurs via influences of innervating neurons. Analogously, we demonstrate that prediction error related activity in the human striatum adapts to the momentarily available reward magnitude and this effect is driven by changes in neuronal dynamics associated with different reward magnitudes.

Reward prediction errors act as a teaching signal for learning (4) and accounts for a wide range of situations (8, 13, 28, 29), including perceptual learning (30). Adaptive coding of prediction errors enables an enhanced discriminability to remain sensitive for mismatches of all sizes. This optimizes efficient coding in neural circuits with given limitations, namely its coding ranges. In a case where PEs were computed based on reward magnitude, learning would be much more sensitive to high rewards while relatively small rewards would not lead to learning. Adaptive coding of reward prediction errors allows the brain to flexibly learn across different reward magnitudes and disturbances in this system would lead to deficits in learning and decision making.

Previous animal studies have provided evidence of neuronal adaptation in coding different aspects of reward. Whereas midbrain dopaminergic neurons adaptively code reward prediction errors (7), OFC neurons show adaptive coding of reward preference (15). OFC neurons also adapt their firing range according to the momentarily available reward range and distribution of rewards (16, 17). Furthermore, recently it has been shown that the primate lateral intraparietal cortex codes saccade values depending on other available choice options. This context-dependence is precisely predicted by the divisive normalization mechanism (31). In humans, fMRI studies have also shown that BOLD signals in reward sensitive areas show magnitude adaptation across possible rewards (14, 32-35).

In our data, we observe significantly less connectivity between the striatum and mPFC/midbrain in high reward compared to low reward conditions (Figure 3C). During the PPI analysis, non-specific correlations across the brain were removed by regressing out the global-mean from every voxel. However, this shifts the correlation distribution to have a mean near zero and forces negative correlations to appear (36-38). Therefore, it is important to interpret only the difference in connectivity between task conditions.

Our PPI results are in accord with previous studies investigating the dynamics of neuronal activation in this anatomic network. The primate striatum is tightly interconnected with the midbrain as well as with cortical areas (18, 39-41). Specifically, the striatum receives dopaminergic input from midbrain regions creating an ascending midbrain-striatal loop (13, 42). Furthermore, PFC activation modulates striatal dopamine release via inhibitory midbrain neurons (43) . More specifically, PFC neurons activate GABAergic cells in the midbrain that in turn inhibit neighbouring dopaminergic neurons projecting to the striatum (44, 45). Thus, one possible pathway underlying our connectivity result is that high magnitudes of reward activate PFC neurons thereby increasing midbrain GABA inhibition, which in turn results in reduced dopamine release in the striatum (46, 47). This pathway may underlie the

adjustment of prediction error signals during high reward outcomes and explain the relative decrease in connectivity between the mPFC/midbrain and the striatum in high vs. low magnitudes.

Taken together, our results provide evidence that adaptive coding of prediction errors in humans is gated by striatal coupling. In line with recordings from primate dopamine neurons (7), we show that striatal prediction errors do not differ for high and low reward magnitudes. Using an effective connectivity analysis, we show that mPFC and midbrain significantly modulate their coupling with the striatum in the face of a high reward magnitude, rendering striatal prediction errors comparable to the lower reward magnitude. Because adaptive prediction errors are essential for learning from high and low rewards this mechanism provides a rich framework within which mechanistic hypotheses for problems such as drug addiction can be examined.

**Materials and Methods**

Experimental Design. In each trial of the task, a reward predicting cue was presented either on the left- or right-hand side of fixation. Subjects were asked to press the corresponding button on a response box as fast as possible. Each cue contained information about both the probability (67% or 33%) and the magnitude (1€ or 10ct) of the possible reward. According to this, there were four different cues, indicating high probability of 1€, low probability of 1€, high probability of 10ct, low probability of 10ct, respectively (Fig. 1*A*). After the button press, a green circle highlighted the stimulus and after a variable inter-stimulus-interval, the outcome cue was presented for 2 seconds. In high reward trials, the outcome was 1€ coin (for received reward) or a red cross superimposed on the 1€ coin (for omitted reward). Analogously, in low reward trials, subjects saw either a 10 ct coin in received trials or a red cross superimposed on the 10 ct coin in omitted trials. The actual reception or omission of reward was determined by the probability indicated by the cue. Subjects performed 5 sessions with 60 trials each. 33 healthy subjects were tested in the study. 5 subjects were excluded from the sample (one due to extreme head movement during scanning [more than 3mm or 3 degrees], three subjects aborted the scanning because they felt sick, one subject was left handed), resulting in a final sample size of n = 28 (13 females and 15 males, mean ± std age = 25.04 ± 2.5).

Behavioral data analysis. To monitor subjects' attention to the task, we analysed the percentage of correct responses. All following analyses included only the correctly responded trials. We examined whether subjects established reward expectations during the reward predicting cue by testing whether reaction time (RT) are influenced by both reward magnitude and probability. For this, we computed a two-by-two (magnitude x probability) ANOVA with repeated measures on RT data.

fMRI data acquisition and preprocessing. Functional imaging was conducted on a 3-Tesla Siemens Trio (Erlangen, Germany) scanner with a 12-channel head coil. In each of the five runs, 366 T2*-weighted gradient-echo echo-planar images (EPI) containing 37 slices (3 mm thick) separated by a gap of 0.75 mm were acquired. Imaging parameters were as follows: repetition time (TR) 2000 ms, echo time (TE) 30 ms, flip angle 70°, matrix size 64x64 and 192 mm field of view, voxel size 3 by 3 by 3.75 mm. A T1-weighted and a T2-weighted structural data set were collected for the purpose of anatomical localization. The parameters were as

follows; T1: TR 1900 ms, TE 2.52 ms, matrix size 256x256, FOV 256 mm, 176 slices (1mm thick), flip angle 9°; T2: TR 8170 ms, TE 0.93 ms, matrix size 256x256, FOV 256 mm, 48 slices (3mm thick), flip angle 120°.

Functional data were analyzed using SPM5 (Wellcome Department of Imaging Neuroscience, Institute of Neurology, London, UK). Images were slice time corrected, realigned, spatially normalized to a standard T2* template of the Montreal Neurological Institute (MNI), resampled to 3 mm isotropic voxels and spatially smoothed using an 8 mm full width at half maximum Gaussian kernel. All included subjects moved less than the size of a single voxel (3mm).

Model-based fMRI data analysis. We computed a general linear model (GLM) with a parametric design (48) to identify brain regions coding prediction errors in an adaptive fashion. In each trial *t*, the prediction error δ was defined as:

$$\delta = r_t - p_t, \quad (1)$$

where $r_t$ is the reward outcome (1 for received and 0 for omitted outcomes) and $p_t$ is the expected probability of the reward (0.33 or 0.66). Note that the task is not a learning task, because the reward probability and magnitudes were explicitly shown and did not change over the experiment. Four regressors were included in the GLM in the following order; 1) onset of the cue, 2) onset of the outcome 3) parametric modulation of the outcome (coded as one when received and minus one when omitted), 4) parametric modulation of the trial-wise prediction errors. The prediction-error regressor was created by parametrically modulating the stimulus function of the outcome by the normalized (mean = 0, SD = 1) trial-wise prediction errors. All regressors were convolved with a canonical hemodynamic response function (HRF). Individual contrast images were computed for prediction-error related responses and taken to a second-level mixed effect analysis using voxel-wise one-sample t-tests.

Reward magnitude dependent changes in striatal connectivity. We performed a whole brain "psycho-physiological interaction" (PPI) analysis (12, 13, 49) with the striatum as a seed region. Here, the entire time series over the experiment was extracted from each subject in the clusters of the striatum, in which activity significantly correlated with PE on the group level. To create the PPI regressor, we multiplied the normalized time series with two condition vectors containing ones for 6 TRs after each reward-magnitude type (one regressor for high and one for low magnitudes) and zeros otherwise. The method used here relies on correlations in the observed BOLD time-series data and makes no assumptions about the nature of the neural event contributing to the BOLD signal (13). The time window of 6 TRs (12 seconds) was selected to capture the entire hemodynamic response function, which peaks after 3 TRs and is back at baseline about 8 TRs after stimulus onset. These PPI regressors were used as covariates in a separate PPI-GLM, in which the following regressors were included; 1) cue onset, 2) psychological regressor accounting for high and 3) low reward outcomes, 4) physiological regressor, (i.e. the entire time series of the seed region over the whole experiment), 5) the PPI regressor for high reward outcomes and 6) the PPI regressor for low reward outcomes. The onset regressors were convolved with an HRF. The resulting parameter estimates of the two PPI regressors represent the extent to which activity in each voxel correlates with activity in the striatum for each condition. Individual contrast images for functional connectivity during high vs. low reward magnitude were then

computed and entered into one-sample t-test. We then identified voxels with significant connectivity during low vs. high reward magnitude.

We applied an omnibus threshold for all whole-brain analyses of $P<0.001$, uncorrected with a cluster extent threshold of k=10 (whole brain results are shown in Table S1 and Table S2). Correction for multiple comparisons (P<0.05, family-wise error (FWE) correction) was then performed for clusters surviving this threshold using 12mm spheres around previously reported peak voxels (small volume correction (SVC)): For the ventral striatum; [-8, 8, -4] and midbrain; [8, -18, -20] from (6) , mPFC; [3, 54, -15] from (25). All reported coordinates (x y z) are in the MNI space.

**Acknowledgements:** This work was supported by the Excellence Initiative of the German Federal Ministry of Education and Research (DFG Grants GSC86/1-2009 and EXC 302), the Max Planck Society, and the Swiss National Science Foundation (SNF 100014_130352).

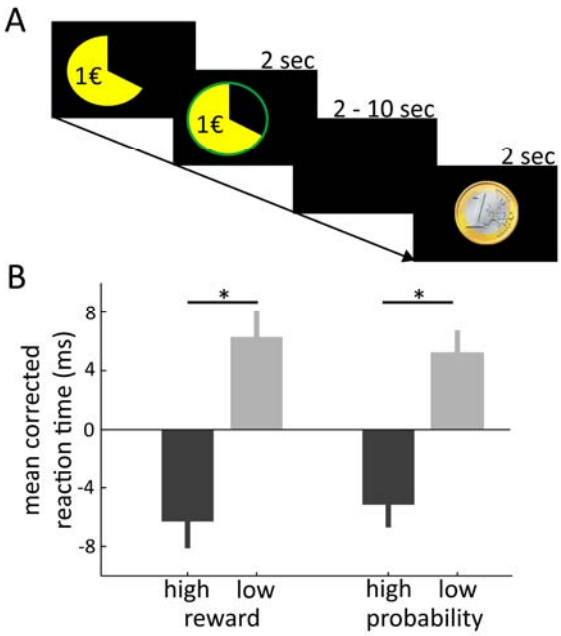


**Figure 1.** Task description and behavioural data.

**(A)** In each trial, subjects saw a visual cue indicating the reward magnitude and probability on the left or right side of the screen. Subjects indicated the location of the cue using a button press, after which a green circle surrounded the cue. After a variable delay, the reward outcome was shown to the subjects.

**(B)** Mean corrected reaction time. Left two bars stand for high and low reward magnitudes and right two bars, for high and low reward probabilities. The greater the reward magnitude, and the higher the probability, the faster the subjects responded. Error bars are s.e.m.

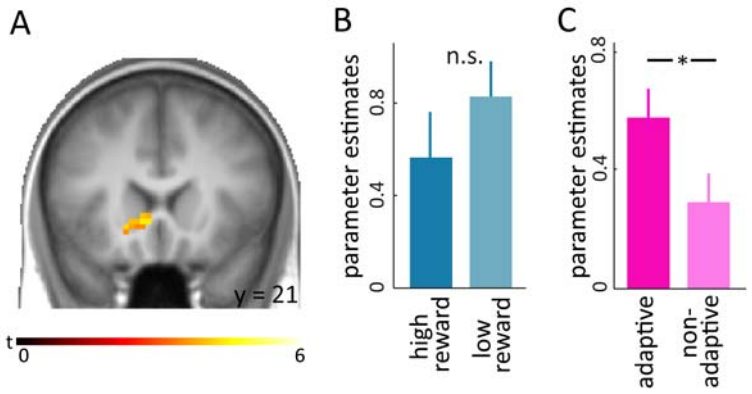


**Figure 2.** Adaptive coding of prediction errors in the striatum.

**(A)** Parametric modulation with trial-wise prediction error revealed significant correlation with BOLD responses in the striatum.

**(B)** Across different reward magnitudes, no significant difference in PE related responses was observed ($t_{27}$=-0.98, *P*=0.34), confirming an adaptive coding of striatal PE. Y-axis represents the parameter estimates of prediction error. Errorbars indicate s.e.m.

**(C)** Adaptive PE predicted striatal BOLD response significantly better compared to non-adaptive PE ($t_{27}$=2.82, *P*=0.0089). Y-axis represents the parameter estimates of prediction error. Errorbars indicate s.e.m.

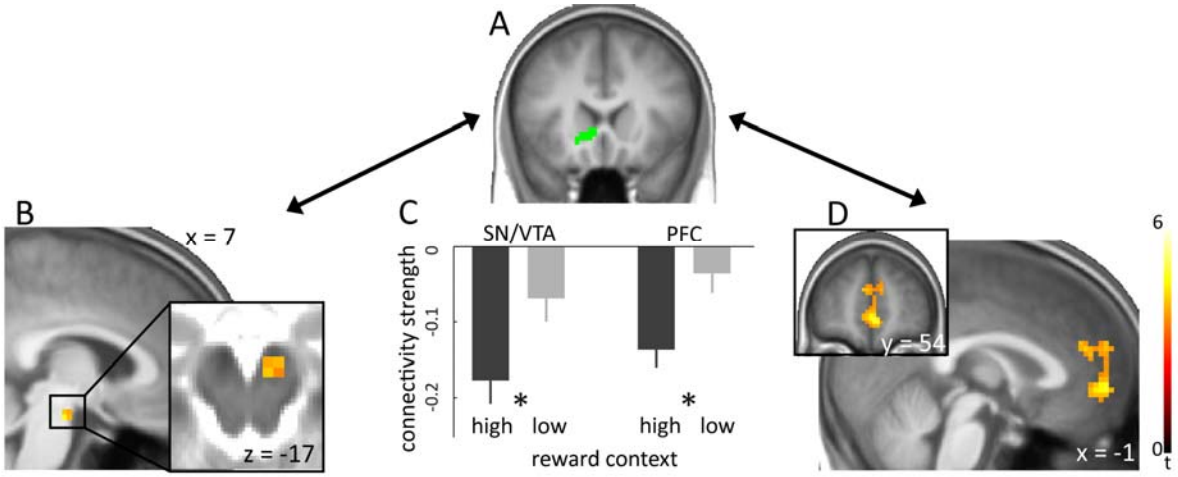


**Figure 3.** Striatal coupling gates adaptive coding of prediction error

**(A)** The striatum showing adaptive coding of prediction errors was used as seed region in the functional connectivity analysis.

**(B)** SN/VTA (box: activity superimposed on T2-weighted image) and **(D)** vmPFC (box: a coronal view) showing significant magnitude-dependent connectivity modulation with the striatum.

**(C)** Bar graph depicts significantly less midbrain-striatal and fronto-striatal connectivity during high compared to low reward magnitudes. Errorbars indicate s.e.m.

## Reference List

1. Tversky A, Kahneman D (1974) Judgment under Uncertainty: Heuristics and Biases. *Science* 185:1124-1131.

2. Kahneman D, Tversky A (1979) Prospect Theory - Analysis of Decision Under Risk. *Econometrica* 47:263-291.

3. Rescorla RA & Wagner AR (1972) A theory of pavlovian conditioning: variations in the effectiveness of reinforcement and nonreinforcement. In *Classical Conditioning II: Current Research and Theory*, eds Black AH & Prokasy WF, (Appleton Century Crofts, New York), pp 64-99.

4. Sutton, R. & Barto, A. (1998) *Reinforcement Learning: An Introduction* (MIT Press, Cambridge, MA).

5. Schultz W, Dayan P, Montague PR (1997) A neural substrate of prediction and reward. *Science* 275:1593-1599.

6. Bayer HM, Glimcher PW (2005) Midbrain dopamine neurons encode a quantitative reward prediction error signal. *Neuron* 47:129-141.

7. Tobler PN, Fiorillo CD, Schultz W (2005) Adaptive coding of reward value by dopamine neurons. *Science* 307:1642-1645.

8. Pessiglione M et al. (2006) Dopamine-dependent prediction errors underpin reward-seeking behaviour in humans. *Nature* 442:1042-1045.

9. Pagnoni G, Zink CF, Montague PR, Berns GS (2002) Activity in human ventral striatum locked to errors of reward prediction. *Nat Neurosci* 5:97-98.

10. McClure SM, Berns GS, Montague PR (2003) Temporal prediction errors in a passive learning task activate human striatum. *Neuron* 38:339-346.

11. O'Doherty JP et al. (2003) Temporal difference models and reward-related learning in the human brain. *Neuron* 38:329-337.

12. Park SQ et al. (2010) Prefrontal cortex fails to learn from reward prediction errors in alcohol dependence. *J Neurosci* 30:7749-7753.

13. Kahnt T et al. (2009) Dorsal Striatal-midbrain Connectivity in Humans Predicts How Reinforcements Are Used to Guide Decisions. *J Cogn Neurosci*.

14. Breiter HC et al. (2001) Functional imaging of neural responses to expectancy and experience of monetary gains and losses. *Neuron* 30:619-639.

15. Tremblay L, Schultz W (1999) Relative reward preference in primate orbitofrontal cortex. *Nature* 398:704-708.

16. Padoa-Schioppa C (2009) Range-adapting representation of economic value in the orbitofrontal cortex. *J Neurosci* 29:14004-14014.

17. Kobayashi S, Pinto de CO, Schultz W (2010) Adaptation of reward sensitivity in orbitofrontal neurons. *J Neurosci* 30:534-544.

18. Haber SN, McFarland NR (1999) The concept of the ventral striatum in nonhuman primates. *Ann N Y Acad Sci* 877:33-48.

19. Kahnt T, Heinzle J, Park SQ, Haynes JD (2010) The neural code of reward anticipation in human orbitofrontal cortex. *Proc Natl Acad Sci U S A* 107:6010-6015.

20. Philiastides MG, Biele G, Heekeren HR (2010) A mechanistic account of value computation in the human brain. *Proc Natl Acad Sci U S A* 107:9430-9435.

21. Ferry AT, Ongur D, An X, Price JL (2000) Prefrontal cortical projections to the striatum in macaque monkeys: evidence for an organization related to prefrontal networks. *J Comp Neurol* 425:447-470.

22. Ongur D, Price JL (2000) The organization of networks within the orbital and medial prefrontal cortex of rats, monkeys and humans. *Cereb Cortex* 10:206-219.

23. Park SQ, Kahnt T, Rieskamp J, Heekeren HR (2011) Neurobiology of value integration: when value impacts valuation. *J Neurosci* 31:9307-9314.

24. Kahnt T, Heinzle J, Park SQ, Haynes JD (2011) Decoding different roles for vmPFC and dlPFC in multi-attribute decision making. *Neuroimage* 56:709-715.

25. Fairhall AL, Lewen GD, Bialek W, de Ruyter van Steveninck RR (2001) Efficiency and ambiguity in an adaptive neural code. *Nature* 412:787-792.

26. Brenner N, Bialek W, de Ruyter van SR (2000) Adaptive rescaling maximizes information transmission. *Neuron* 26:695-702.

27. Dunn FA, Lankheet MJ, Rieke F (2007) Light adaptation in cone vision involves switching between receptor and post-receptor sites. *Nature* 449:603-606.

28. O'Doherty JP, Buchanan TW, Seymour B, Dolan RJ (2006) Predictive neural coding of reward preference involves dissociable responses in human ventral midbrain and ventral striatum. *Neuron* 49:157-166.

29. Behrens TE, Hunt LT, Woolrich MW, Rushworth MF (2008) Associative learning of social value. *Nature* 456:245-249.

30. Kahnt T, Grueschow M, Speck O, Haynes JD (2011) Perceptual learning and decision-making in human medial frontal cortex. *Neuron* 70:549-559.

31. Louie K, Grattan LE, Glimcher PW (2011) Reward value-based gain control: divisive normalization in parietal cortex. *J Neurosci* 31:10627-10639.

32. Elliott R, Agnew Z, Deakin JF (2008) Medial orbitofrontal cortex codes relative rather than absolute value of financial rewards in humans. *Eur J Neurosci* 27:2213-2218.

33. Nieuwenhuis S et al. (2005) Activity in human reward-sensitive brain areas is strongly context dependent. *Neuroimage* 25:1302-1309.

34. Bunzeck N, Dayan P, Dolan RJ, Duzel E (2010) A common mechanism for adaptive scaling of reward and novelty. *Hum Brain Mapp* 31:1380-1394.

35. Lohrenz T, McCabe K, Camerer CF, Montague PR (2007) Neural signature of fictive learning signals in a sequential investment task. *Proc Natl Acad Sci U S A* 104:9493-9498.

36. Van Dijk KR et al. (2010) Intrinsic functional connectivity as a tool for human connectomics: theory, properties, and optimization. *J Neurophysiol* 103:297-321.

37. Murphy K et al. (2009) The impact of global signal regression on resting state correlations: are anti-correlated networks introduced? *Neuroimage* 44:893-905.

38. Fox MD, Zhang D, Snyder AZ, Raichle ME (2009) The global signal and observed anticorrelated resting state brain networks. *J Neurophysiol* 101:3270-3283.

39. Haber SN, Kunishio K, Mizobuchi M, Lynd-Balta E (1995) The orbital and medial prefrontal circuit through the primate basal ganglia. *J Neurosci* 15:4851-4867.

40. Haber SN, Fudge JL, McFarland NR (2000) Striatonigrostriatal pathways in primates form an ascending spiral from the shell to the dorsolateral striatum. *J Neurosci* 20:2369-2382.

41. Haber SN, Knutson B (2010) The reward circuit: linking primate anatomy and human imaging. *Neuropsychopharmacology* 35:4-26.

42. Ikemoto S (2007) Dopamine reward circuitry: two projection systems from the ventral midbrain to the nucleus accumbens-olfactory tubercle complex. *Brain Res Rev* 56:27-78.

43. Frankle WG, Laruelle M, Haber SN (2006) Prefrontal cortical projections to the midbrain in primates: evidence for a sparse connection. *Neuropsychopharmacology* 31:1627-1636.

44. Sesack SR, Deutch AY, Roth RH, Bunney BS (1989) Topographical organization of the efferent projections of the medial prefrontal cortex in the rat: an anterograde tract-tracing study with Phaseolus vulgaris leucoagglutinin. *J Comp Neurol* 290:213-242.

45. Sesack SR, Pickel VM (1992) Prefrontal cortical efferents in the rat synapse on unlabeled neuronal targets of catecholamine terminals in the nucleus accumbens septi and on dopamine neurons in the ventral tegmental area. *J Comp Neurol* 320:145-160.

46. Karreman M, Westerink BH, Moghaddam B (1996) Excitatory amino acid receptors in the ventral tegmental area regulate dopamine release in the ventral striatum. *J Neurochem* 67:601-607.

47. Karreman M, Moghaddam B (1996) The prefrontal cortex regulates the basal release of dopamine in the limbic striatum: an effect mediated by ventral tegmental area. *J Neurochem* 66:589-598.

48. Buchel C, Holmes AP, Rees G, Friston KJ (1998) Characterizing stimulus-response functions using nonlinear regressors in parametric fMRI experiments. *Neuroimage* 8:140-148.

49. Friston KJ et al. (1997) Psychophysiological and modulatory interactions in neuroimaging. *Neuroimage* 6:218-229.